University of Wisconsin Milwaukee
UWM Digital Commons

Theses and Dissertations

August 2022

Interaction Between Test Structure and Shake Table Powered By Servo-hydraulic Actuation

RONG XU
University of Wisconsin-Milwaukee

Follow this and additional works at: https://dc.uwm.edu/etd

 Part of the Engineering Commons

Recommended Citation

XU, RONG, "Interaction Between Test Structure and Shake Table Powered By Servo-hydraulic Actuation" (2022). *Theses and Dissertations*. 3113.
https://dc.uwm.edu/etd/3113

This Thesis is brought to you for free and open access by UWM Digital Commons. It has been accepted for inclusion in Theses and Dissertations by an authorized administrator of UWM Digital Commons. For more information, please contact scholarlycommunicationteam-group@uwm.edu.

INTERACTION BETWEEN TEST STRUCTURE AND SHAKE TABLE POWERED BY SERVO-HYDRAULIC ACTUATION

by

Rong Xu

A Thesis Submitted in

Partial Fulfillment of the

Requirements for the Degree of

Master of Science

in Engineering

at

the University of Wisconsin-Milwaukee

August 2022

ABSTRACT

INTERACTION BETWEEN TEST STRUCTURE AND SHAKE TABLE POWERED BY SERVO-HYDRAULIC ACTUATION

by

Rong Xu

The University of Wisconsin-Milwaukee, 2022
Under the Supervision of Professor Jian Zhao

This study focused on the interaction between shake tables and test structures. The shake tables are usually powered by servo-hydraulic actuation and under displacement control. The dynamic response of test structures may lower the ability of the shake table to produce motion at the natural frequency of the test structures. Models of the shake table at the Earthquake Engineering Research Center (EERC) and the new table at the Ningbo University of Technology (NBUT) were created in this study. Parametric analyses revealed that the table-structure interaction is affected by the dynamic response speed of the shake tables in addition to other known factors such as structural properties and table control parameters. The adverse impact of table-structure interaction increases with an increase in the mass of test structure and a decrease in its damping. When the natural frequency of the test structure is within the working frequency bandwidth of the shake table, the table may still be able to generate ground motion that can cause large responses in the test structure; however, when the structures' natural frequency is outside the bandwidth, the test structure may not be able to develop sufficient responses to the simulated earthquakes.

© Copyright by Rong Xu, 2022
All Rights Reserved

To

my family and my friends

TABLE OF CONTENTS

LIST OF FIGURES

LIST OF TABLES

ACKNOWLEDGEMENTS

First, I would like to sincerely thank Prof. Jian Zhao for his guidance and patience. "Learn how to ask questions and learn how to ask long questions." This was a great piece of advice from Prof. Zhao, throughout my graduate study. I would like to thank Prof. Yue Chen at NBUT for his help in my thesis and guidance in my life.

I would like to appreciate Frank Liu, Qian Lin and other UWM students for their help during my graduate studies, for taking me out to have a good view of Wisconsin in a three-dimensional way, and for understanding American culture from a different dimension. I would also like to thank Tina sincerely for caring for me while I was living in Milwaukee.

I would like to sincerely thank Ningbo University of Technology to give me financial support for the research. Professor Kejian Cai (Front Dean of Civil Engineering in NBUT), Professor Shuichao Zhang (Dean of Civil Engineering in NBUT) allowed me as a graduate student and provided resources for my graduate study. I am grateful to Professor Qing Lv for providing test data that is presented in this thesis. Mr. Qin from Servotest answered many of my questions. Without their help, I would not be able to finish this study.

I am also grateful for the internship opportunity given by Shanghai Municipal Engineering Design Institute, which helped me to find enthusiasm and the light for my future. Thanks to Jinxin Bu for his professional help.

Finally, I would like to thank my family and all my friends for their support and encouragement along the whole way. My three year of master's degree was very special, experiencing the COVID-19 and the different educational environment between the US and

China. There were times of pain, self-doubt, and avoidance, but more importantly, I have grown up from these experiences. I appreciate all the help from everyone in my life.

Chapter 1. Introduction

1.1 Table-structure Interaction

Shaking tables are a powerful tool for seismic engineering research. For example, the Ningbo University of Technology (NBUT) recently acquired a shake table from Servotest Testing Systems Ltd., capable of producing six degrees of freedom ground motion to test structures. The table is supported by four vertical actuators and four horizontal actuators to accommodate such input (Fig. 1.1). Although eight hydraulic actuators are installed, the two horizontal actuators in X-direction can be used to generate horizontal ground motion in this direction. The complex hydraulic actuation of the table can be simplified as one uni-directional actuator driving the table as illustrated in Fig. 1.2. This study focused on the behavior of shake tables in one horizontal direction.

The NBUT shake table weighs 15.5 tons and has a frequency of 145 Hz (high stiffness is required), and for structural testing are driven by servo-hydraulic actuation (Fig. 1.2). The actuators were controlled by individual servovalve, which is in turn controlled by a controller. The servovalve controller compares command signals to feedback signal, resulting a direct current (DC) error. An electrical signal proportional to the DC error is then sent to the servovalves to drive the valve spools during a test. The spool position controls hydraulic flow into the actuators, resulting in a difference in fluid pressure across the pistons. The forces delivered to the shake table is thus the pressure difference multiplied by the piston area. A displacement sensor on the table measured its displacement, which was then transmitted back to the servovalve controller to close the control loop if the shake table is under displacement control.

The control signal can also be generated by acceleration feedback signal if the table is under acceleration control. Finally, the control signal can contain both DC errors from the table displacement and table acceleration if the table is under mixed control [7]. The pilot stage of servovalve for NBUT's shake table system is SV80, meaning 80 L/min rated flow and the main stage is SV500 (500 L/min or 132 gpm). In addition, horizontal hydraulic actuators are type 080-250-100 with $\pm$ 125 mm strokes. More detailed information related servo hydraulic system could be found in [14].

Fig. 1.3 shows a single degree of freedom (SDOF) structure with a weight of 6.5 tons and a natural frequency around 7 Hz. This elastic specimen was designed and manufactured by Ningbo University of Technology and Servotest to demonstrate its feasibility. This structure is fixed on the table, which means there is no flexibility between the table and the SDOF structure. This SDOF structure was used for (1) earthquake time wave reproduction accuracy test; (2) system frequency response curve test; and (3) other tests that need to be done per the request. For example, for the system frequency response tests, a random signal with a bandwidth of 1 to 50 Hz is generated; an iterative Control System (ICS) was used to generate the command file.

NBUT shake table is mainly under displacement control. The experimental determination of the system transfer function or weighting function involves finding the function which, when convoluted with the auto correlogram of input, will most closely fit the cross-correlogram between the input and output signals. The experimental transfer functions were determined with data obtained by personal communication with Prof. Lv in Fig. 1.4. The black solid lines represent the shake table with a 6.5-ton SDOF structure whose fundamental frequency is 7 Hz; the blue dashed lines show the table with a 20-ton weight; the red dotted lines are for the bare table.

Note that in order to improve the table response, the operators must pre-amplify the command signal as illustrated in Fig. 1.5.

From the experimental transfer function of table with SDOF structure in Fig.1.4, the table cannot produce ground motion (in terms of ground acceleration) near the natural frequency of the test structure. The inability to produce the simulated ground motion is the maximum at the natural frequency of the test structure. This is caused by table-structure interaction (Rinawi et al. 1991). However, the observed table-structure interaction is different from that observed by precious researchers, including Rinawi et al.. The amplitude shows the severe dip around the natural frequency of SDOF structure. However, the manifestation of frequency response amplitude is “peak and notch” in other researchers’ reports [3,6,8,9]. Besides, the key to shaking table tests is to reproduce sufficient ground motion, especially at the natural frequency of test structures to cause damage to the test structures. Therefore, it is necessary to figure out what would cause and plays role in this table-structure interaction in frequency response.

1.2 Research Objectives

The objective of this research was to investigate the interaction between test structures and the shake table powered by servo-hydraulic actuation. Specifically, the objectives are:

(1) To develop an analytical model for a shake table model that includes the feedback control loops and devise methods to identify the model parameters.

(2) To reproduce the results of Rinawi et al. (1991) using the shake table at the Earthquake Engineering Research Center (EERC).

(3) To identify critical parameters to the table-structure interaction for shake tables under displacement feedback control.

(4) To do parametric analysis and study sensitivity of key indicators for table-structure interaction.

(5) To verify the speed of NBUT's servo hydraulic shaking table system can be critical to table-structure interaction.

This thesis is organized as follows: a literature review is provided in Chapter 2. A mathematical model is established in Chapter 3 to explain the table-structure interaction. Chapter 4 contains numerical models for typical shake tables powered by servo-hydraulic actuation under displacement control. The models were established based on a simple shake table at EERC. The common manifestation of the distortion in frequency response is shown in Chapter 4. In addition, the different table-structure interaction experimenting from NBUT's shake table is provided. With parameters determined based on a report by Rinawi and Clough (1991), a parametric study was presented in Chapter 5 to show the impact of critical parameters on table-structure interaction. The FFT responses are also provided to explain structural properties in Chapter 5. Summary and conclusion are shown in the last chapter in this thesis, including a future study at the end.

Chapter 2 Literature Review

Blondet et al. (1988) [10] first observed the loss of fidelity in reproducing the reference signal and developed an analytical model for a uniaxial shake table loaded with single degree of freedom (SDOF) structures with displacement feedback control. Fig. 2.1 shows the effect of structure properties on frequency response of SDOF system. Blondet proposed the concept of table-structure interaction and pointed out that the dynamic response of the system is distorted in a frequency range centered on the natural frequency of the test structure as a result of table-structure interaction, which is so-called peak-and-notch effects as shown in Fig. 2.1. Table-Structure Interaction in frequency response is peak and notch amplitude accompanied by a violent phase lag, which means the reproduction of a dynamic signal or ground motion is imperfect [1-3]. This interaction effects were apparent around the natural frequency of the test structure ($\boldsymbol{\omega_{st}}$). At a frequency slightly below $\boldsymbol{\omega_{st}}$, the table output is amplified (called resonance), and when the driving frequency is equal to $\boldsymbol{\omega_{st}}$, the most severe attenuation (called antiresonance) is created. As a result of table-structure interaction, the response of seismic simulators degrades more with increasing structure/system mass and resonant frequency ratios and less with increasing structural damping. In addition, Blondet concluded that the physical parameters of both the seismic simulator and the test structure are important since the interaction between the shaking table and the structure is essentially mechanical. Therefore, it appears necessary to investigate the key components of the interaction problem in increasingly intricate systems from a mechanical standpoint.

Rinawi et al. (1991) [3] considered two different cases in his mechanical models of the shake table at the earthquake Engineering Research Center (EERC): first is the base of the

structure is completely fixed, which means there is no flexibility between the table and base. And the second is the structure and the table acting as a coupled system. Several simplified methods for dealing with the interaction effects were proposed, and these consist mainly of adding springs and dampers to the base of the structure to account for shaking table flexibilities. Mechanical models (Rocking and horizontal flexibility model) that are customary to provide an additional spring and damper to represent the horizontal soil flexibility, dealing with the interaction effects.

Control-Structure Interaction (CSI) effects were first proposed to improve the performance and stability of systems in 1995 (Dyke et al.) [6]. It is demonstrated that a hydraulic actuator's dynamic properties are intimately coupled to the dynamics of the structure to which it is attached by a natural velocity feedback relationship. Neglecting this feedback interaction might result in the controlled system performing poorly, depending on how well the actuator-structure interaction dynamics are described. Consider the case in which the system has one actuator, with a single command input $\boldsymbol{u}$ generating a single output force $\boldsymbol{f}$. Fig. 2.2 provides a block diagram description of this case that the model of interaction between the actuator and the structure. And the transfer function $\boldsymbol{H_i}$ presents dynamics between the structure and actuators. Therefore, the overall transfer function from valve command $\boldsymbol{u}$ to the structural response $\boldsymbol{y}$ is given by $\boldsymbol{G_{yu}} = \frac{\boldsymbol{G_{yf}G_a}}{\boldsymbol{1+G_{yf}G_aH_i}}$. However, the transfer function from the command to the external force applied to the structure is shown as following: $\boldsymbol{G_{fu}} = \frac{\boldsymbol{G_a}}{\boldsymbol{1+G_{yf}G_aH_i}}$.

It is obvious that the dynamics of the connection from $\boldsymbol{u}$ to $\boldsymbol{f}$ include dynamics resulting from the structure and the actuator in addition to actuator dynamics. The performance of the controlled system is greatly enhanced by taking actuator dynamics and control-structure interaction into

consideration when designing a controller, which is widely used in other later researchers' analytical models.

The shaking table system task is to reproduce a certain displacement input history. To achieve this goal, the system continually compares the command signal with the table displacement and applies a correction proportional to the difference between the two signals. Therefore, control system model intended to represent the shaking table horizontal interaction during the tests at the earthquake engineering research center at Berkeley, CA (EERC). The author concluded for the case if the bare table and the table with stiff mass, it is noted that the interaction effects are insignificant. Fig. 2.3 shows transfer functions of table horizontal displacement over horizontal command displacement where there are no interaction effects in amplitude curve (dashed line for bare table situation). While using a table horizontal command signal, a shift in the horizontal table motion's frequency component close to the structural frequency was seen.

Conte et al. (2000) [9] explained that the design of physical system parameters, the characteristics of the control loop(s), and the features of the test structure are a few examples of the many variables that affect how much distortion occurs during signal reproduction. Conte et al. built a linear analytical model that is a singled-directional, servo-hydraulic, displacement feedback controlled shaking table system, and a thorough investigation of the table sensitivity with regard to all relevant system (including proportional, integral, derivative and differential pressure gains of the control system) and payload parameters (incorporating flexibility of SDOF payloads) is done. Fig. 2.4 shows the main effect of changing PID control gains: the larger proportional gain is, the bigger magnitude of the transfer function in the low-medium frequency

range (0-60 Hz); more increased the derivative gain is, the larger the amplitude of the oil column peak is and the smaller the oil column frequency is. Fig. 2.5 presents the same result in papers [3,10] that the distortion (peak-and-notch) occurs at the natural frequency of SDOF system with a fixed base. Similarly, Conte JP et al. also made the conclusions [3,10] that for a given natural frequency, the payload peak and notch distortion increases in size for decreasing payload damping and increasing payload weight. In generally, Proportional-integral-differential (PID) controllers are often utilized to displacement control the hydraulic actuators used in shaking table tests. Displacement control, however, typically results in unsatisfactory acceleration tracking in the time domain and insufficient reproducibility of produced accelerations (Nakata, 2010). Therefore, acceleration control of shake tables is proposed to improve the shaking tables' acceleration tracking capabilities.

In summary, table-structure interaction causes a distortion at the natural frequency of one or multiple DOF structures no matter in displacement feedback control or acceleration feedback control. Although Rinawi et al. in EERC report concluded the peak and notch behavior have less of an impact on the system responsiveness than was previously believed, Ryu et al. (2016) [15] still insist that it is crucial to reproduce signals with accuracy, especially for shake table certification tests, whose primary goal is to confirm a given level of performance of test structures or equipment, have more strict restrictions in order to subject the specimens to predetermined target movements. Ryu pointed out the transfer function would be distorted if a specimen mounted on a shake table and developed a shake table-nonlinear hysteretic structure system model. The author first presented the relation between the input, the desired shake table displacement $\boldsymbol{x_d}$, and the output, the measured displacement of shake table $\boldsymbol{x_t}$, shown as in Fig.

2.6. A mathematical model of a shake table-structure system is introduced, and the specimen mounted on the table presented in Fig. 2.6 is a nonlinear hysteretic SDOF structure. The equations in time domain could be described as following:

$$\boldsymbol{m_s\ddot{x}_s(t) + c_s\dot{x}_s(t) + f_S(\underline{x}) = -m_s\ddot{x}_t(t)}$$

$$\boldsymbol{m_t\ddot{x}_t(t) - \{c_s\dot{x}_s(t) + f_S(\underline{x})\} = f_a(t)}$$

$$\boldsymbol{\dot{f}_S(\underline{x}) = k_T(\underline{x})\dot{x}_s(t)}$$

$$\boldsymbol{k_a x_d(t) = \frac{1}{{\omega_a}^2}\frac{\dot{f}_a(t)}{m_t} + \frac{2\zeta_a}{\omega_a}\frac{f_a(t)}{m_t} + \dot{x}_t(t) + k_a x_t(t)}$$

Where $\boldsymbol{\omega_a, \zeta_a, and\ k_a}$ are the natural frequency, the equivalent damping ratio, and the control gain of the shake table system; $\boldsymbol{f_S(\underline{x})}$ is a nonlinear restoring force, $\boldsymbol{k_T(\underline{x})}$ indicates the instantaneous tangent stiffness.

The above equations could be written in the state space form as $\boldsymbol{\dot{\underline{x}}_t(t) = f(\underline{x}_t(t), u(t))}$. Where $\boldsymbol{u(t) = x_d(t)}$, and for the output $\boldsymbol{y(t)}$ of the total acceleration response $\boldsymbol{\ddot{x}_s^t(t) = \ddot{x}_s(t) + \ddot{x}_t(t)}$ at the top of the structure, the output equation is $\boldsymbol{y(t) = -m_s^{-1}\{c_s\dot{x}_s(t) + f_S(\underline{x})\}}$. The table-structure interaction could be seen from this equation.

Matthew et al. (2014) discussed the table-multiple degree of freedom test structure dynamic relationship in another way, using transfer function matrix to understand this dynamic relationship. The model used in his paper shown in Fig. 2.7, a single directional shake table loading a linear MDOF structure. Matthew et al. provided system transfer function matrix from the shake table and the displacement of test structure to the external forces applied to the table as following: $\begin{bmatrix} G_{fx}^{ss}(s) & G_{fx}^{st}(s) \\ G_{fx}^{ts}(s) & G_{fx}^{tt}(s) \end{bmatrix} \begin{bmatrix} X_{st}(s) \\ X_t(s) \end{bmatrix} = \begin{bmatrix} 0 \\ F_t(s) \end{bmatrix}$

Where $\boldsymbol{G_{fx}^{ss}(s)}$ is the transfer function if the test structure; $\boldsymbol{G_{fx}^{st}(s)}$ and $\boldsymbol{G_{fx}^{ts}(s)}$ are the transpose transfer function matrices; $\boldsymbol{G_{fx}^{tt}(s)}$ is the transfer function of the shaking table. Therefore, the following is the transfer function that directly connects the actuator force and shaking table displacement:

$$\boldsymbol{F_t(s) = \left(G_{fx}^{tt}(s) - G_{fx}^{ts}(s) \left(G_{fx}^{ss}(s) \right)^{-1} G_{fx}^{st}(s) \right) X_t(s) = G_{f_t x_t}(s) X_t(s).}$$

The inverse of the above equation yields the following relationship, which describes the output (displacement of shaking table) from an input (actuator force applying to the table): $\boldsymbol{X_t(s) = \frac{1}{G_{f_t x_t}(s)} F_t(s) = G_{x_t f_t}(s) F_t(s)}$, demonstrating the relationship between external force and shaking table displacement, $\boldsymbol{G_{x_t f_t}(s)}$ herein, is influenced by shaking table characteristics and structure properties. So, what is the table-structure interaction is illustrated again here in another perspective.

For the tracking control of a shake table, various compensation methods have been proposed to eliminate the interaction effects to some extent. Researchers Nakata [16] and Phillips and Spencer [17] and others have recently introduced feedforward compensation methods combined with real-time feedback loops to reduce tracking error. These methods use outer feedback loops (i.e., the term outer is used to differentiate the feedback loop from the inner feedback loop of actuators) to reduce tracking error rather than the offline iteration approach. Experiments demonstrating high agreement between the target and the output helped to validate the methodology. In order for a nonlinear hysteretic structure's output response to adhere to a predetermined goal motion, Ryu et al. (2016) formulated, based on the

feedback linearization approach, a real-time nonlinear feedback tracking controller and a technique was proposed to establish the control excitation input of a shaking.

From precious researchers' studies, table-structure interaction is presented as the distortion of table output in the frequency domain. Therefore, figuring out the nature of table-structure interaction effects in another mathematic way would be a focus of my study to further understand the distortion in amplitude curve. Besides, if the manifestation of table-structure interaction is always a narrow peak and notch under displacement control would be discussed in this thesis. Since table structure interaction is a wide and deep dip in frequency response when the SDOF structure with 7Hz loaded on NBUT's shake table.

Chapter 3. Mathematical Models

3.1 Introduction

Transfer function, all the initial conditions assumed to be zero, is a great tool for analyzing the linear and time-invariant system. Fig. 3.1 presents the general transfer functions of my analytical model for table-structure system, involving hydraulic actuator, test structure and displacement feedback controller. In addition, the mathematic process of table structure interaction would be also introduced in this chapter.

3.2 Influence of Test Structure on Table Output

Fig. 3.1 describes the schematic of transfer functions for bare table system with displacement feedback control. $\boldsymbol{G_t(s)}$ is used to present the transfer function of bare table

$$\boldsymbol{G_t(s)} = \frac{\boldsymbol{s}}{\boldsymbol{M_t s^2 + C_t s}} \tag{3.1}$$

Shake tables usually do not have components that provide restoring forces, as illustrated in Fig. 3.2. Fig. 3.2 shows for the free body diagrams of two separated sub-structures: the shake table and SDOF structure on the table. the equilibrium equations of are

$$\boldsymbol{M_{st}\ddot{x}_{st} + C_{st}\dot{x}_{st} + K_{st}x_{st} = K_{st}x_t + C_{st}\dot{x}_t} \text{ for the structure,} \tag{3.2}$$

$$\boldsymbol{M_t\ddot{x}_t + C_t\dot{x}_t + K_{st}x_t + C_{st}\dot{x}_t = K_{st}x_{st} + C_{st}\dot{x}_{st} + F} \text{ for the table} \tag{3.3}$$

where, $\boldsymbol{M_{st}, K_{st}, C_{st}}$ is mass, stiffness and damping of single degree of freedom structure respectively; $\boldsymbol{M_t, C_t}$ is mass, and damping of shaking table respectively; $\boldsymbol{x_{st}, \dot{x}_{st}, \ddot{x}_{st}}$ is the displacement, the first-order derivative of displacement and the second-order derivative of displacement of test structure respectively; $\boldsymbol{x_t, \dot{x}_t, \ddot{x}_t}$ is the displacement, the first-order derivative of displacement and the second-order derivative of displacement of shaking table

respectively; $\boldsymbol{F}$ is an external force applied on the shaking table by actuators. Note that both set of vectors have the same reference point at the fixed ground.

Eq. 3.3 can be rewritten in matrix form:

$$[\boldsymbol{M}]\begin{bmatrix}\ddot{x}_{st}\\ \ddot{x}_t\end{bmatrix}+[\boldsymbol{C}]\begin{bmatrix}\dot{x}_{st}\\ \dot{x}_t\end{bmatrix}+[\boldsymbol{K}]\begin{bmatrix}x_{st}\\ x_t\end{bmatrix}=\begin{bmatrix}0\\ F\end{bmatrix} \tag{3.4}$$

where,

$[\boldsymbol{M}]=\begin{bmatrix}\boldsymbol{M_{st}} & \boldsymbol{0}\\ \boldsymbol{0} & \boldsymbol{M_t}\end{bmatrix}$is the mass matrix,$[\boldsymbol{C}]=\begin{bmatrix}\boldsymbol{C_{st}} & \boldsymbol{-C_{st}}\\ \boldsymbol{-C_{st}} & \boldsymbol{C_t+C_{st}}\end{bmatrix}$ is the damping matrix, and$[\boldsymbol{K}]=$ $\begin{bmatrix}\boldsymbol{K_t} & \boldsymbol{-K_{st}}\\ \boldsymbol{-K_{st}} & \boldsymbol{K_{st}}\end{bmatrix}$is the stiffness matrix.

Eq. (3.4) could be expanded to write as following,

$$\begin{bmatrix}M_{st} & 0\\ 0 & M_t\end{bmatrix}\begin{bmatrix}\ddot{x}_{st}\\ \ddot{x}_t\end{bmatrix}+\begin{bmatrix}C_{st} & -C_{st}\\ -C_{st} & C_{st}+C_t\end{bmatrix}\begin{bmatrix}\dot{x}_{st}\\ \dot{x}_t\end{bmatrix}+\begin{bmatrix}K_t & -K_{st}\\ -K_{st} & K_{st}\end{bmatrix}\begin{bmatrix}x_{st}\\ x_t\end{bmatrix}=\begin{bmatrix}0\\ F\end{bmatrix}. \tag{3.5}$$

Eq. (3.5) could be written in the frequency domain with Laplace transform, producing the system transfer function from the shaking table and test structural displacement to applied forces from horizontal actuator, and the relationship could be written as (3.6)

$$\left(\begin{bmatrix}M_{st} & 0\\ 0 & M_t\end{bmatrix}\boldsymbol{s^2}+\begin{bmatrix}C_{st} & -C_{st}\\ -C_{st} & (C_{st}+C_t)\end{bmatrix}\boldsymbol{s}+\begin{bmatrix}K_t & -K_{st}\\ -K_{st} & K_{st}\end{bmatrix}\right)\begin{bmatrix}X_{st}(s)\\ X_t(s)\end{bmatrix}=\begin{bmatrix}0\\ F(s)\end{bmatrix}. \tag{3.6}$$

Eq. 3.6 could also be written as the following equation:

$$\begin{bmatrix}M_{st}s^2+C_{st}s+K_{st} & -C_{st}s-K_{st}\\ -C_{st}s-K_{st} & M_ts^2+(C_{st}+C_t)s+K_{st}\end{bmatrix}\begin{bmatrix}X_{st}(s)\\ X_t(s)\end{bmatrix}=\begin{bmatrix}0\\ F(s)\end{bmatrix}. \tag{3.7}$$

The table displacement can be obtained by solving Eq. 3.7, and the ratio of this displacement to the applied force (by the hydraulic actuation) is defined as the transfer function of the table loaded with an SDOF structure. Fig. 3.3 shows the block diagram of table-structure system. Block $\boldsymbol{G_{st}(s)}$ presents table-structure interaction, and the transfer function of $\boldsymbol{G_{st}(s)}$ in the frequency domain could be written as following:

$$G_{st}(s) = \frac{x_t}{F} = \frac{(M_{st}s^2+C_{st}s+K_{st})}{[M_ts^2+(C_{st}+C_t)s+K_{st}](M_{st}s^2+C_{st}s+K_{st})-(C_{st}s+K_{st})^2}. \quad (3.8)$$

Eq. 3.8 indicates that the actuator force cannot produce desired table response at the natural frequency of the test structure. That is the reason why there is a valley at the natural frequency of test structures in frequency response curve. As for the explanation of the peak in the interaction effects happening below the natural frequency of DOF structures, we need to have a look at the poles of denominator in Eq. 3.8. The numerical method could be used to figure out the reason for the peak in frequency response. If the poles are smaller than the zeros at numerator, a peak would happen before a valley. It is exactly the situation we observed the distortion in magnitude response under displacement control. We will discuss it in detail in Chapter 4 after all parameters are determined.

3.3 Table-Structure Interaction

The block diagram of a shaking table system with SDOF test structures for closed displacement feedback control is presented in Fig. 3.3. Related transfer functions of each block presented in Fig. 3.3 is discussed in more details in this section. The governing differential equations of a typical servo-hydraulic actuator can be found in Zhao (2003); hence only the transfer functions are presented below:

$\boldsymbol{CF}$ is the transfer function of signal conversion, conversion factor, turning command signal (ground displacement or ground acceleration) to voltage signal. The input is DC error (e) that is the subtraction between command signal and feedback signal and v, the input of Proportional-Proportional-Integral (PID) controller, is the actual command (valve command) sending to servovalve. The dynamics of internal PID controller is simplified as a constant $\boldsymbol{G_P}$, using

proportional gain only in study throughout. $\boldsymbol{G_v(s)}$ is the transfer function of servovalve dynamics and $\boldsymbol{G_f(s)}$ presents the valve flow. The valve dynamics is described in as:

$$\boldsymbol{G_v(s) = \frac{0.1}{\tau s+1}} \tag{3.9}$$

Where $\boldsymbol{\tau}$ is the system time delay, presenting the response delay of the servovalve.

Time delay means the actuator piston position lags the valve command. The servovalve time delay values can change both the amplitude and frequency of the oil column peak in amplitude curve (Conte, 2000). Therefore, it is necessary to be considered in this analytical model. With a certain piston position, hydraulic flow is injected in one side of actuator chamber and the other side is open to zero-pressure return line. The dynamics is simplified as a flow gain. $\boldsymbol{K_v}$ is the initial no-load flow gain, a proportional gain for the servovalve flow and spool opening if considering the nonlinearities of flow are negligible. Fig. 3.5 shows the nonlinear flow model, a typical flow VS Spool opening curve. The slope of Fig. 3.5 defines $\boldsymbol{K_v}$, and the flow gain decreases when the spool opening increases in practice. However, the nonlinear flow gain is usually not apparent since servovalves are frequently thought of as proportional. More information about nonlinearities in servovalve could be found in [14].

The velocity of the actuator piston/test structure affects the load pressure, and the force ($\boldsymbol{F}$) delivered to the shake table is equal to the load pressure multiplied by the piston are ($\boldsymbol{P_L A}$); hence, the applied force is impacted by the structural velocity response. The transfer function of actuator is shown in Equation 3.10.

$$\boldsymbol{G_a(s) = \frac{A}{K_a s+Cl}} \tag{3.10}$$

Where $\boldsymbol{K_a = {V}/{4\beta_e}}$ is the compressibility coefficient of the hydraulic fluid inside both actuator chambers, in which $\boldsymbol{V}$ is volume of actuator chambers and $\boldsymbol{\beta_e}$ is effective oil modules, and $\boldsymbol{C_l}$ is the total leakage coefficient of the servovalve/actuator combination, $\boldsymbol{A}$ is the piston area of rod in actuators.

The transfer function $\boldsymbol{G_t(s)}$ of shake table is given in Eq. 3.1, meaning bare table; while transfer function $\boldsymbol{G_{st}(s)}$ presented in Eq. 3.8 is table-structure system. $\boldsymbol{G_{at}(s)}$ presents the transfer function of natural velocity feedback, forming a closed loop for actuator and table-structure for table-structure system (Fig. 3.3) or for actuator and table for bare table system (Fig. 3.1).

$$\boldsymbol{G_{at}(s) = \frac{G_a(s)\times G_{st}(s)}{1+G_a(s)G_{st}(s)\times A} = 1 + \frac{A^2 s\left(M_{st}s^2+C_{st}s+K_{st}\right)}{(K_a s+Cl)(-(C_{st}s+K_{st})^2+(M_{st}s^2+C_{st}s+K_{st})(M_t s^2+(C_{t+}C_{st})s+K_{st}))}} \quad (3.11)$$

If we want to study the relation in a bare table system, use $\boldsymbol{G_t(s)}$ instead of $\boldsymbol{G_{st}(s)}$ when writing $\boldsymbol{G_{at}(s)}$. $\boldsymbol{G_{at}(s)}$ is similar to the control-structure-interaction (CSI) that first appeared in Dyke's paper (1995). More details related to CSI could be found in paper (Dyke, 1995).

Next, it is determined how the reference and measured shaking table displacements correspond to one another overall. Eq. 3.12 describes the overall transfer function of bare table system for displacement- controlled system and Eq. 3.13. is for table-structure system.

$$\boldsymbol{G_{d\_bare}(s) = \frac{G_s(s)G_{pid}(s)G_v(s)G_f(s)s)G_{at}(s)/s}{1+G_s(s)G_{pid}(s)G_v(s)G_f(s)s)G_{at}(s)/s} = \frac{0.1ACFG_pK_v}{0.1A\,CFG_pK_v+s(Cl+K_as)(C_t+M_ts)(1+T_ds)+A^2s(1+sT_d)}} \quad (3.12)$$

$$\boldsymbol{G_{d\_TS}(s) = \frac{G_s(s)G_{pid}(s)G_v(s)G_f(s)s)G_{at}(s)/s}{1+G_s(s)G_{pid}(s)G_v(s)G_f(s)s)G_{at}(s)/s} =}$$

$$\boldsymbol{\frac{0.1ACFG_pK_v(M_{st}s^2+C_{st}s+K_{st})}{0.1A\,CFG_pK_v(M_{st}s^2+C_{st}s+K_{st})+s(Cl+K_as)(M_{st}s^2+C_{st}s+K_{st})+(K_{st}(M_t+M_{st})s)+s(C_{st}(M_{st}+M_t)+sM_{st}M_t)(1+T_ds)+A^2s(1+sT_d)(M_{st}s^2+C_{st}s+K_{st})}} \quad (3.13)$$

There is no table-structural interaction effects on bare table system (no information of structure at numerator of Eq. 3.12); however, it is clear that table-structure interaction happens in Eq. 3.13.

Table 3.1 shows all parameters for the EERC shake table from Rinawi et al. (1991) and the NBUT shake table system. The parameter identification is discussed in Chapter 4. Here the manifestation of table-structure interaction, peak and notch, is presented, showing its predictability. Fig. 4.3 in blue solid line is the frequency response from analytical model applied EERC's data (Table 3.1), showing a valley at structural natural frequency (2.87 Hz) and a peak before the valley. Fig. 4.4 presents the transfer function of Table-Structure system for NBUT's data. The notch still happens at natural frequency of SDOF structure, while the peak is not obvious.

3.4 Summary and Discussion

The uni-axial shake table loaded with single degree of freedom (SDOF) test structure is derived in this chapter. The dynamics of the hydraulic actuator, displacement feedback control and table-structure interaction were all incorporated in the formulas. Table-structure interaction is presented in mathematical method. Transfer functions of each block in analytical model are described in detail in Fig. 3.3 and would be discussed in later chapters. In addition, two different analytical models are used to verify the notch frequency happening as in overall system's transfer function. Therefore, understanding the mathematic process in this Chapter helps to predict peaks and valleys.

Chapter 4. Parameter Identification

4.1 Introduction

MATLAB SIMULINK models were used to reproduce the results observed by Rinawi et al. (1991) with EERC's shake table. Parameter identification is also contained based on EERC's report in this chapter. We will use two key indicators and compare analytical results with experimental results from previous researchers to verify the correctness of analytical models in SIMULINK.

4.2 SIMULINK Model

Block diagrams are often more convenient for revealing relationships between individual components, such as the effect of the piston/structure velocity on the actuator dynamics. First, the dynamic relationships for shaking tables, including electro-hydraulic actuators, table platform, test structures, and typical feedback control systems, are introduced at the very beginning. Block diagrams of displacement feedback control table-structure system shown in Fig. 3.3, including actuator dynamics, servovalve, feedback controller. In this model, the shake table is assumed to be operating in displacement control with a conventional proportional-integral-derivative (PID) controller.

4.3 Parameter Identification

Table 3.1 presents all parameters of the EERC's servo hydraulic table-structure system and NBUT's. After the preliminary establishment of the model, the method to verify whether the model is correct can be to use the experimental data in the EERC report to verify and compare the analysis results of my model with those data in EERC's report. There are three cases: bare table, table loaded with $\mathbf{70}\ \boldsymbol{kips}$ weight, table loaded with $\mathbf{68.4}\ \boldsymbol{kips}$ SDOF payload.

Parameters identifying for bare table condition is based on the EERC's report [3]. Some parameters are available from the report directly, including the servo valve type, actuator type, damping, mass, and the weight of the shake table and test structure. So, I could know the area of the actuator movable rod ($\boldsymbol{A}$), the stoke of the actuator movable rod ($\boldsymbol{L}$), the rated flow of the servo valve from technic documents, and $\boldsymbol{K_v}$ (the initial no-load flow gain) could be calculated from rated flow. However, there are several parameters that are not directly available from the report, so I made a reasonable guess, and it is necessary to verify those hypothetical parameters by comparing key indicators later, including out-of-phase frequency, bandwidth in frequency response. These hypothetical parameters include $\boldsymbol{Ka}$ (the compressibility coefficient of the hydraulic fluid inside both actuator chambers), $\boldsymbol{Cl}$ (leakage coefficient of the servosystem) and Proportional gain ($\boldsymbol{P\ gain}$)in this study, and the assumption of values based on Zhao (2003).

Random signals were used for structural identification in EERC's report. The frequency and damping of fixed-base case are $\boldsymbol{2.87\ Hz}$ and $\boldsymbol{0.3\ percent}$ respectively; and are $\boldsymbol{2.5\ Hz}$ and $\boldsymbol{3.33\ percent}$ respectively in coupled table-structure case. However, the report pointed out that "Much larger damping values were determined from the earthquake tests than were observed in the random signal tests with the small shaker. These damping values increased with the amplitude of earthquake excitation and this significant change in damping can be attributed to the fact that the mass was not rigidly attached to the structure." So, the damping value would be a bit different with EERC's shake table.

At last, $\boldsymbol{Mst}$ is $\boldsymbol{68.4\ kips}$, $\boldsymbol{Kst}$ is $\boldsymbol{57.9\ kips/in}$ and $\boldsymbol{Mt = 100\ kips}$, damping ratio of table is $\boldsymbol{30}\%$. I consider the mass of foundation under test structure in case 3 (i.e., table loaded

with $\mathbf{68.4}\ \boldsymbol{kips}$ SDOF test structure) and I set structural damping as $\mathbf{2}\%$. EERC also provides the natural frequency of SDOF structure that is $\mathbf{2.87}\ \boldsymbol{Hz}$.

In addition, there are some other parameters that need to make sure in my model. Finally, my parameters setting is time delay $\boldsymbol{Td = 15ms}$, compressibility coefficient $\boldsymbol{Ka = 1.191(in^3/ksi)}$, main-stage valve null flow gain $\boldsymbol{Kv = 1894.6(in^3/sec/\%)}$, leakage coefficient $\boldsymbol{Cl = 23}$ $\boldsymbol{(in^3 - ksi/sec)}$, table mass in bare table case is $\boldsymbol{Mt = 0.2588(kips - sec^2/in)}$, but is $\boldsymbol{0.305(kips - sec^2/in)}$ in case 3 (foundation mass is considered). Table horizontal stiffness $\boldsymbol{Kt = 401(kips/in)}$, table damping coefficient $\boldsymbol{Ct = 6.126(kips - sec^2/in)}$ (considering damping ratio of table is 30%), stiffness of test structure $\boldsymbol{Kst = 57.9(kips/in)}$, damping of test structure $\boldsymbol{Cst = 0.128(kips - sec^2/in)}$. It is necessary to give a detailed and credible description of the values of these parameters, showing in Table 3.1.

Time delay Td

This parameter is not an accurate value from experimental process. So the reasonable guess is here for the complete analytical model. Time delay is set as 15 ms to represent the servovalve dynamics (Zhao, 2003) whose servovalve used $\boldsymbol{MTS\ 256.09}$ with $\mathbf{90}\ \boldsymbol{gpm}$ flow capacity. However, the type of the servovalve in EERC table is similar but with a flow capacity of $\mathbf{170}\ \boldsymbol{gpm}$,. So, Td is assumed as $\mathbf{15}\ \boldsymbol{ms}$ here.

Compressibility coefficient $\boldsymbol{Ka}$

Ka is a constant related to actuators. $\boldsymbol{Ka = \frac{V_t}{4\beta_e}}$, is the compressibility coefficient of the hydraulic fluid inside both actuator chambers. $\boldsymbol{V_t}$, the total chamber volume, is determined by the piston area $(\boldsymbol{A})$ of the rod and the total stroke $(\boldsymbol{l})$ of the actuator. So, $\boldsymbol{V_t}$ equals $\boldsymbol{A}$ times $\boldsymbol{l}$. In

reality, stroke would be a bit longer than the value in technic documents due to piston rod end stuff, so I amuse the stoke is $\mathbf{13}\ \boldsymbol{in}$ here instead of $\mathbf{12}\ \boldsymbol{in}$. And the piston area was $\mathbf{25.4}\ \boldsymbol{in^2}$ in EERC's report. As for effective bulk modulus $\boldsymbol{\beta_e}$, substantially lowered by entrained air and mechanical compliance is assumed as about $\mathbf{69.3}\ \boldsymbol{ksi}$ here. Therefore, Ka is calculated as $\mathbf{1.191}(\boldsymbol{in^3/ksi})$.

Main-stage valve null flow gain $\boldsymbol{Kv}$

$\boldsymbol{Kv}$, a technical parameter, is the third-stage flow gain. However, servovalve model of EERC's is too ancient to know this parameter. So, I assume it is proportional with EFT's based on models from two papers both belong to MTS company. The valve in EFT's model has $\mathbf{90}\ \boldsymbol{gpm}$ flow and $\boldsymbol{Kv}$ is 1003$(\boldsymbol{in^3/sec}/\%)$. So, it is reasonable to set $\boldsymbol{Kv}$ as $\mathbf{1894.6}(\boldsymbol{in^3/sec}/\%)$ that is 1.89 times as EFT' since valve flow is $\mathbf{170}\ \boldsymbol{gpm}$ in EERC's, which is about 1.89 times of EFT's.

Leakage flow Cl

Leakage flow $\boldsymbol{Cl}$ exists because the clearance between circular actuator piston rings and their sleeve forms an annular flow passage. It is difficult to determine the specific value of leakage coefficient in practice since the leakage was related to the level of wornness of the equipment such as the piston sealing. Anyway, I guess $\boldsymbol{Cl} = \mathbf{23}\ (\boldsymbol{in^3 - ksi/sec})$ according to analytical results.

Table mass $\boldsymbol{Mt}$

Table mass is $\mathbf{100}\ \boldsymbol{kips}$ in EERC, $\mathbf{100}\ \boldsymbol{kips}$ directly used in bare table case and weighted mass case but considered the foundation weight on shake table in SDOF structure case. Therefore,

table mass set as $\mathbf{0.305}(\boldsymbol{kips} - \boldsymbol{sec^2/in})$ in case 3($\mathbf{118}\ \boldsymbol{kips}$ of shake table, involving foundation weight), which means here are around $\mathbf{18}\ \boldsymbol{kips}$ foundation on shake table.

Table damping coefficient $\boldsymbol{Ct}$

Table damping coefficient could be calculated $\boldsymbol{Ct} = \mathbf{6.126}(\boldsymbol{kips} - \boldsymbol{sec^2/in})$ according to table horizontal stiffness value $\mathbf{401}\ \boldsymbol{kips/in}$ from EERC, which means there are $\mathbf{30}\ \boldsymbol{percent}$ damping ratio of this table.

Parameters of NBUT's are provided by the table operator, Mr. Qin from Servotest and technical documents based on known servovalve type and actuators type, shown in Table 3.1. Note that $\boldsymbol{Kv}$ is assumed linear and is set as $\mathbf{1361.41}(\boldsymbol{in^3/sec}/\%)$ which is 1.6 times of maximum flow ($\boldsymbol{Q_{max}}$) based on assumption.

4.4 Verification of the models

Conte (2000) pointed out a thorough investigation of the table sensitivity with regard to all relevant system and payload parameters is required to optimize the physical characteristics and the control gain settings for optimum accuracy in motion reproduction by the table under a variety of payload situations [9]. We know the information about the table and test structure from EERC's report, so we could verify the accuracy of parameters and the system models. There are some key indicators need to be matched to verify the models presented in Chapter 3, including the out-of-phase frequency (frequency at which the phase is 180 degrees), 3dB bandwidth. This section points out two key indicators and get the similar results from analytical models and EERC's experimental data. Besides, sensitivity analysis of structural properties (structural mass and structural damping) has done and the comparison between analytical data and experimental data also offers evidence to the correctness of the models.

Out-of-phase frequency

The black dotted line in Fig. 4.1 shows the transfer function from command displacement to actual displacement from experimental data of EERC's bare table situation by random signals. The out-of-phase frequency is 10.2 Hz, which actually is the same as oil column frequency. Out-of-phase frequency is the frequency in phase curve, while oil column frequency is got from amplitude curve. Blue solid line in Fig. 4.1 shows the transfer function for bare table from my analytical model. It is obvious the oil column frequency is similar, around 10 Hz.

In addition, oil column frequency could be calculated by known parameters, given by [4, 8]. So, the exact out-of-phase frequency is got by calculating the oil column frequency as following:

$$\boldsymbol{f_{oil} = \frac{A}{\pi}\sqrt{\frac{\beta}{Vm_t}} = \frac{25.4}{\pi}\sqrt{\frac{100\ (ksi)}{25.4\ (in^2) \times 10\ (in) \times \left(\frac{100}{386.4}\right)(kips - sec^2/in)}} = 9.97\ (Hz)}$$

The calculated value is very close to the experimental data and analytical data. Fig. 4.2 and Fig. 4.3 represent transfer functions of another two conditions: additional fixed weighted mass on table and table loaded with SDOF structure. The main effect of these twos cases is that additional mass on table would decrease the oil column frequency.

The transfer function of oil column frequency from the external force to the displacement of shaking table could be deduced as following:

$$\boldsymbol{G_{oil}(s) = \frac{Cl + K_a s}{s(A^2 + ClC_t + C_t K_a s + K_a M_t s^2)} = \frac{C_l + K_a s}{K_a s\left(M_t s^2 + \left(c_t + \frac{C_l M_t}{k_a}\right)s + \frac{A^2 + C_t C_l}{K_a}\right)}}$$

The transfer function of oil column frequency presents the results for open loop dynamics of the system, which means the gain in displacement feedback closed loop is zero. Besides, from this equation above, we know all parameters except for proportional gain of PID controller that

we would make sure by matching 3dB bandwidth of system could be ensured since the indicator out-of-frequency we addressed preciously matches with the result from EERC's.

3 dB bandwidth

The adjustment of proportional gain mainly affects $\boldsymbol{3\ dB}$ bandwidth. Therefore, getting the same frequency bandwidth is the method to make sure $\boldsymbol{Pgain}$ $(\boldsymbol{G_p})$ value herein. The purpose of reproduce the same transfer functions of EERC's as maximum extent as possible for all three different situations is make verification of parameters setting in analytical models. Because transfer function reflects the system reproduction of the command signal and is a crucial method to examine the shake table's performance.

Fig. 4.1 describes the bare table situation. $\boldsymbol{3\ dB}$ bandwidth is 10.95 Hz for EERC's transfer function, which is very close to the bandwidth of my analytical model 11.03 Hz. Fig. 4.2 shows the additional 70 kips weight fixed on the table. $\boldsymbol{3\ dB}$ bandwidth is different in this case though; the trend is the same which is additional mass lower the frequency bandwidth. Fig. 4.3 presents the transfer function of table-structure system, which means the SDOF structure loaded on shaking table. $\boldsymbol{3\ dB}$ bandwidth is almost the same in this case. In addition, there is an obvious interaction happening at the natural frequency of test structures. Amplitude of resonance frequency is 2.2 in EERC's model and is 2 in analytical model and amplitude of anti-resonance frequency is both 0.7 in two models, which could reflect the rationality of parameters setting in analytical models. Until now, proportional gain is set as 1.67 reasonably for EERC's model in this analytical model under displacement control.

After making certain all parameters of analytical models, it is necessary to match results between analytical models and experimental data from others' report. Blonde in 1988 and

Clough in 1991 did the similar experiments, trying to explore the relation between structural mass and structural damping and table-structure interaction.

Fig. 4.4 illustrates the effect of changing structural mass on the system transfer function. Black solid line descripts the situation that there is no loaded flexible structure on the table. Red dotted line presents the SDOF structure on the table equals $\mathbf{0.04}$ $(\boldsymbol{kips - sec^2/in})$. Bule dashed line means the heavy structure on the table ($\mathbf{0.34}$ $(\boldsymbol{kips - sec^2/in})$). It is observed that the major effect of boosting the structural mass is to increase the peak magnitude of the transfer function. The notch is getting closer to structural frequencies, while the peak is moving further away from structural natural frequencies. In addition, the oil column frequency is smaller when the structural mass becomes heavier. Generally, the heavier SDOF structure is, the larger size of "peak and notch", including amplitude and frequency range.

Fig. 4.5 describes the effect of changing structural mass on peak and notch value in frequency response. A changing structural mass divided by table mass as the dimensionless abscissa; a changing peak value or notch divided by the amplitude of case 3 (SDOF structural mass =$\mathbf{0}$ $(\boldsymbol{kips - sec^2/in})$) as the dimensionless ordinate. Similarly, while the dashed black line explains the peak sensitivity study to structural mass, the solid black line depicts the notch's effect on various SDOF structural weight. Increasing the mass of loaded structure, has the main effect of enhancing the amplitude of peak before the natural frequency of the structure. The peak boost significantly when the mass of SDOF structure is heavier than the table mass. Red points are from Clough's experimental data and blue points are from Blondet's experimental data. It is clear that experimental data from others get close to the data from analytical models, which

means the correctness of analytical models is great. The same conclusion could be made from analysis of Fig. 4.6 and Fig. 4.7.

The impact of structural damping on the system transfer function is shown in Fig. 4.6. It demonstrates the obvious benefit of having larger structural damping in table-structure system. Black solid line means the damping ratio of structure is 20 percent; red dotted line presents the damping ratio is 5 percent, and blue dashed line shows 1 percent damping ratio. Higher structural damping levels greatly lessen the peak and notch effects. Higher damping levels result in a somewhat reduced table response at higher frequencies. Besides, the effect for influenced frequency range could be neglect.

Fig. 4.7 shows the effect of changing structural damping on peak and notch value. A changing structural damping ratio as the abscissa, from 1 percent to 20 percent; the physical meaning of ordinate is the same as Fig 4.5. The sensitivity of the damping for peak value is significantly larger than that for notch when the damping ratio is minimal. The notch influenced by structural damping is essentially undetectable when the damping ratio is more than 10 percent. Similarly, the experimental data from others match well with analytical models' results.

4.5 General comments on parameter identification

From comparisons of transfer functions for three different cases (Fig. 4.1~Fig. 4.3), analytical models match EERC's experimental results well, especially for those key indicators: out-of-phase frequency and the 3 dB bandwidth frequency in different three situations. In addition, the comparison in sensitivity analysis between analytical models and experimental data from others verify the reliability of analytical models. In this chapter, a simple servo hydraulic shake table-structure system model is developed that could reflect table-structure interaction in frequency

response. Therefore, parametric analysis for NBUT's shake table could be continued in next chapter.

Chapter 5. Parametric Analyses

5.1 Introduction

Analytical models for NBUT could be built once all parameters listed in Table 3.1 are known. From experimental data of shake table in NBUT loaded with 6.5 tons SDOF structure, a wide and deep dip is observed in frequency response (Fig. 1.4), which is different with the distortion (narrowed "peak and notch") occurred in EERC' report (addressed in Chapter 4). Clough concluded that table-structure interaction could be ignored in most cases. This conclusion could be confirmed by Fig. 5.1~ Fig. 5.6. However, the situation is different in NBUT's shake table: the response at natural frequency of SDOF structure is too small to cause damage at last. Parametric analysis of NBUT's shake table is discussed in this chapter.

5.2 Parametric Analysis

The observation in EERC [3] of table structure interaction is the narrow peak and notch in frequency response and made the conclusion that this interaction could be ignored. Fig. 5.1~ Fig. 5.6 support this conclusion because the response at natural frequency of the test structure is as large as expected response. in this section, the same results of EERC would be presented to confirm the conclusion that table structure could be ignored when structure's natural frequency is 2.87 Hz (within the flat range). However, the proportional gain and structure's natural frequency have large impact on table structure interaction. Also, the same analysis for NBUT's shake table are run in this section. But first for the 7 Hz structure and then move to a smaller frequency within the flat range.

If sin sweep (Fig. 5.1) as input sent into the analytical model equipped with EERC's parameters. The black dotted lines in Fig. 5.2 indicate that the relative displacement induced by SDOF structure loaded on the shake table in time domain, while the blue solid line presents the expected response of the structure subjected to the ground motion. Fig. 5.3 provides FFT amplitude response for these two situations. The response of SDOF structure loaded on the table is large enough to cause damage though the response peak occurred at a frequency slightly lower than the natural frequency of the test structure – the impact of table-structure interaction The same observation can be made for the Kobe earthquake (1995) ground motion (Fig. 5.4). The response of SDOF structure in Fig. 5.6 follows the expected displacement of the same structure on the ground directly. However, if the test structure's natural frequency is large outside the flat range (such as 8 Hz), table structure couldn't be neglected. Fig. 5.7~Fig. 5.10 support this conclusion. Fig. 5.7 describes comparison for displacement between structure on the ground and structure (8Hz) on the table in time domain for EERC's table by sending sin sweep reference. In this case, the structure mounted on the table couldn't response as command shown in Fig. 5.8. And the same results would be seen in Fig. 5.9 and Fig. 5.10 by sending Kobe earthquake displacement as input.

The same situation in NBUT's shake table happens: if natural frequency of SDOF structure is outside the flat range, the structural response would be unsatisfactory. Fig. 5.12 and Fig. 5.14 illustrate the response at natural frequency (7 Hz) of SDOF structure is too small to cause the maximum damage. Therefore, the natural frequency of SDOF structure play a significant role in the interaction.

In addition, table-structure interaction should be related to the responding speed of the shake table. Various proportional gain in analytical model is the simplest way to present the system speed.

Proportional Gain

Fig. 5.15 depicts the effect of altering system gain (proportional gain of the PID controller) in analytical model for EERC shake table. Black solid line presents the transfer function for standard analytical model (P-gain equals 1.67) derived in precious chapters, using for comparison. Noting that the mass of table in case 3 (table loaded with SDOF structure) is the sum of table mass and SDOF structure mass. Blue dashed line means the system with unity proportional gain. Red dashed line presents the transfer function of table loaded SDOF structure system with 2 P-gain. We could know from Fig. 5.11 that peak amplitudes typically increase with higher system gain settings, having much more significant effects than notch. Lower gain values tend to attenuate the higher frequencies much faster. In addition, the larger P-gain decline the influenced frequency range.

A changing P-gain as an abscissa in Fig. 5.16; the peak value or notch changing with P-gain divided by the amplitude value of the case for table weighted the same mass as the dimensionless ordinate. So, the ordinate presents the sensitivity of proportional gain (from 1 to 2 herein) resulting in interaction effects. Solid black line shows the notch influenced by various proportional gain, while dashed black line describes the change of peak value with different proportional gain. Red points in Fig. 5.16 are data points from EERC's report. Generally, peak ratio and notch ratio have larger influence in variation range of proportional gain between 1 to 1.5; after value 1.5, peak value is more affected by the P-gain of controller comparing with the notch.

Structural natural frequency

Black solid line in Fig. 5.16 illustrates the transfer function of table loaded with SDOF structure with 2.87 Hz natural frequency from the command displacement to the table's horizontal displacement. Red dashed line is the circumstance that the natural frequency of SDOF structure is 8 Hz and Blue dotted line presents 1 Hz. This graph makes it obvious that there is a considerable peak and notch near the natural frequency of SDOF structure. In addition, a second peak (oil column peak) is seen at frequencies greater than the uncoupled structural natural frequency. Higher structural frequencies result in a wider frequency gap between peak and notch frequencies.

5.3 Analysis for NBUT's Shake Table

Proportional Gain

Fig. 5.18 describes transfer functions of various levels of input for NBUT's analytical models under displacement control. Different levels of input is achieved in SIMULINK models by changing proportional gain, which means the speed of this shake table is changed with the various gain. It is obvious that table-structure interaction should be related to the responding speed of the table. Slower speed of the table results in wider frequency range between the peak and notch frequency. In addition, the faster speed of the table causes lager size of distortion in frequency response. It is obvious that the peak affected by table-structure interaction much more significant than the notch if structural frequency is 7 Hz in Fig. 5.19. However, the situation is different in case that structural frequency is 1 Hz. The impacted frequency is narrow, which is the similar as situation in EERC's analysis shown in Fig 5.20 and Fig. 5.21.

Structural Properties

From comparing Fig. 5.22 and Fig. 5.24, we know the notch always happens at natural frequency of SDOF structure. However, the peak impacted significantly by different structural frequency. As for the situation that the natural frequency of structures is large, the table-structure interaction is suffered easier. Fig. 5.24 demonstrates the case that SDOF structure with small natural frequency has small impacted frequency, and table-structure interaction effect the amplitude response mainly rather than frequency range.

The same results in changing structural damping ratio. Small natural frequency of SDOF structure has less effect on impacted frequency range. In the contrast, large structural frequency will result in huge impacted frequency.

Nonlinear flow gain

Generally, if SDOF structure mounted on the table has large natural frequency, table-structure interaction not only reflect on magnitude response but more on impacted frequency range in frequency response. Fig. 5.30 shows different natural frequency of structures in NBUT's shake table system. The most obvious observation in this figure is large structural frequency has more impacted frequency range that is mainly due to table-structure interaction. In this case, the faster responding speed help a bit to improve the performance of the shake table, which is the behavior that table operator does on NBUT's shake table. However, if system speed is amplified infinitely, nonlinearity of servovalve would come into the servo hydraulic system (shown in Fig. 3.5). Too much amplification of input signal means too much spool opening, which result in the nonlinearity of servovalve. The emergence of nonlinearity would exacerbate table-structure interaction at last.

Fig. 5.31 shows the FFT amplitude response in NBUT's analytical model considering nonlinearity of servovalve. The blue line is the expected response, while the solid line is the actual response. It is obvious that the response is very small especially at the natural frequency of SDOF structure. Fig. 5.32 presents the input is amplified four times and the expected response is amplified by 4 times. However, the actual response of SDOF structure is only 2 times than before, which means the responding speed is smaller.

Chapter 6. Summary and Conclusions

6.1 General conclusions

In this study, models were created to study the interaction between a test structure and a shake table. Such interaction, observed in previous studies in the literature, has been signatured as a narrow notch around the natural frequency of the test structure and a narrow peak at a smaller frequency in the frequency domain. The notch indicates that shake tables cannot generate ground motion at the natural frequency of the test structure, leading to low table fidelity; however, the peak near the frequency may compensate such adverse impact such that the table may generate sufficient ground motion that causes nonlinear behavior of test structures.

The table-structure interaction, observed in the shake table at the Ningbo University of Technology, however, appears much more severe that those in the literature. In the frequency domain, the inability of the shake table to produce ground motion around the natural frequency of a test structure cross a wide frequency; and no apparent peak was observed.

Models were created for the NBUT shake table as a single direction and displacement-controlled servo-hydraulic system in MATLAB SIMULINK. The model comprises of analytical equations for the transfer functions between input (command signal: ground displacement) and output (the actual table displacement). The proposed model has the benefit of including servovalve time delay, foundation mass, the connection between the shake table and test structures, closed-form system, in contrast to earlier work on shake table modelling by other researchers. In order to conduct a thorough sensitivity analysis respecting the proportional gain of the displacement feedback table PID controller, the test structure properties, and damping

ratio of shake table, a shake table model was built based on analytical-experimental data of EERC's table. In summary, this single-directional, servo-hydraulic actuator controlled, closed-form feedback (displacement-controlled system) discussed in this study reveals:

(1) The table-structure interaction is affected by the dynamic speed of the shake table in addition to other known factors such as structural mass and damping ratio of structures.
(2) Faster speed of shake table narrows the impacted frequency range of the T-S interaction.
(3) The table-structure interaction is affected by the natural frequency of SDOF structure mounted on the table.
(4) Larger natural frequency of SDOF structure has wider impacted frequency range in T-S interaction.
(5) Amplification of command signal could get close to the desired response. However, infinite amplification of reference would induce nonlinearity of servovalve.
(6) The emergence of nonlinearity of servovalve exacerbates T-S interaction.

6.2 Future Work

When shake tables are loaded with specimens, especially the test structures are heavy and high, the interaction between the tables and structures influences the system dynamics that may result in unexpected performance. Many compensation methods have been widely proposed and used in terms of table controls nowadays and most of them assume that the specimens loaded on the table keep linear during shake table tests, such as feedforward compensation with real-time feedback loops, a real-time feedback control scheme, TVC control system etc. However, when heavy and flexible specimens behave nonlinearly during tests, inferior signal performances are seen. Considering nonlinearity in different compensation

methods could be studies in depth in the near future. Besides, nonlinear behaviors of servovalve actuator dynamics, of oil column in the actuator chamber could be considered when deriving mathematical formulas and setting up the analytical block diagrams.

Reference

[1]. Rea D, Abedi-Hayati S, Takahashi Y. Dynamic analysis of electro-hydraulic shaking tables. EERC Report No. 77/29, Earthquake Engineering Research Center, University of California at Berkeley, CA, 1977.

[2]. Hwang JS, Chang KC, Lee GC. The system characteristics and performance of a shaking table. NCEER Report No. 87-0004, National Center for Earthquake Engineering Research, State University of New York at Bufalo, NY, 1987.

[3]. Rinawi AM, Clough RW. Shaking table-structure interaction. EERC Report No. 91/13, Earthquake Engineering Research Center, University of California at Berkeley, CA, 1991.

[4]. Trombetti TL. Experimental/analytical approaches to modeling, calibrating and optimizing shaking table dynamics for structural dynamic applications. Ph.D. Dissertation, Department of Civil Engineering, Rice University, Houston, TX, 1998.

[5]. Luco JE, Ozcelik O, Conte JP. Acceleration tracking performance of the UCSD-NEES shake table. Journal of Structural Engineering 2010; 136(5):481–490. doi:10.1061/(ASCE)ST.1943-541X.0000137.

[6]. Dyke SJ, Spencer BF Jr, Quast P, Sain MK. The role of control–structure interaction in protective system design. Journal of Engineering Mechanics 1995; 121:322–338.

[7]. MTS System Corporation. Real Time Hybrid Seismic Test System – User's Manual. MTS Systems Corporation, Minneapolis: USA, 2004.

[8]. Muhlenkamp M, Conte JP, Hudgings TR, Durrani AJ. Analysis, design, and construction of a shaking table facility. Structural Research at Rice, Report No. 46, Department of Civil Engineering, Rice University, Houston, TX, 1997.

[9]. Conte JP, Trombetti TL. Linear dynamic modeling of a uniaxial servo-hydraulic shaking table system. Earthquake Engineering and Structural Dynamics 2000; 29(9):1375–1404

[10]. Blondet M, Esparza C. Analysis of shaking table-structure interaction effects during seismic simulation tests. Earthquake Engineering and Structural Dynamics 1988; 16(4):473–490.

[11]. Ozcelik O, Luco JE, Conte JP, Trombetti TL, Restrepo JI. Experimental characterization, modeling and identification of the NEES-UCSD shake table mechanical system. Earthquake Engineering and Structural Dynamics 2008; 37(2):243–264.

doi:10.1002/eqe.754.

[12]. Maddaloni G, Ryu KP, Reinhorn AM. Simulation of floor response spectra in shake table experiments. Earthquake Engineering and Structural Dynamics 2010; 40(6):591–604. doi:10.1002/eqe.1035.

[13]. Blondet M, Esparza C. Analysis of shaking table-structure interaction effects during seismic simulation tests. Earthquake Engineering and Structural Dynamics 1988; 16(4):473–490.

[14]. Zhao J. Development of EFT for nonlinear SDOF systems.[D]. University of Minnesota. 2003.

[15]. Ki P. Ryu, Andrei M. Reinhorn, Real-time control of shake tables for nonlinear hysteretic systems, Structural Control and Health Monitoring, 10.1002/stc.1871, 24, 2, (e1871), (2016).

[16]. Nakata N. Acceleration tracking control for earthquake simulators. Engineering Structures 2010; 32(8):2229–2236. doi:10.1016/j.engstruct.2010.03.025.

[17]. Phillips BM, Spencer Jr BF. Model-based framework for real-time dynamic structural performance evaluation. NSEL Report No. NSEL-031, Urbana-Champaign, Illinois, 2012.

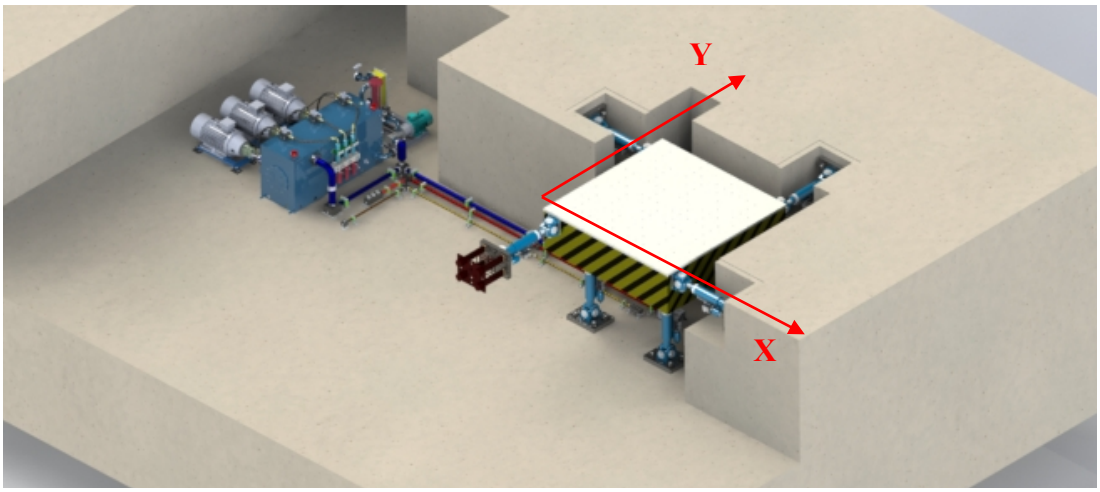

Figure 1.1 The overview of actuators position[1]

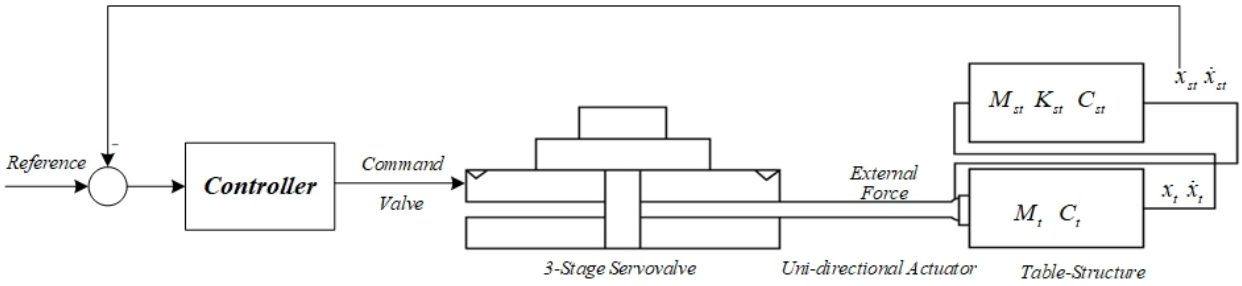

Figure1.2 Simplified shake table system with one horizontal actuator

Figure 1.3 Shake table with SDOF payload in NBUT

[1] This photo is provided by ServoTest Company.

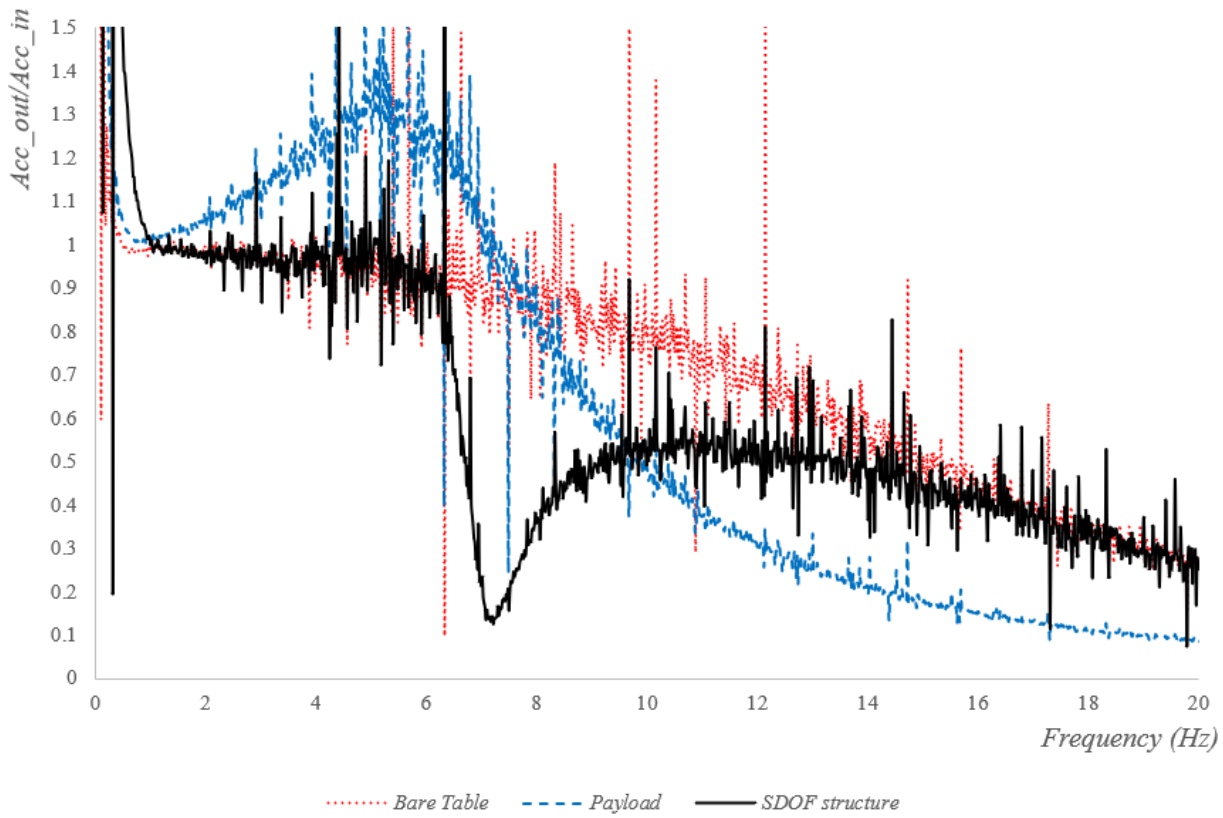

Figure 1.4 Transfer functions of three situations (Bare table, payload and table loaded with SDOF structure)

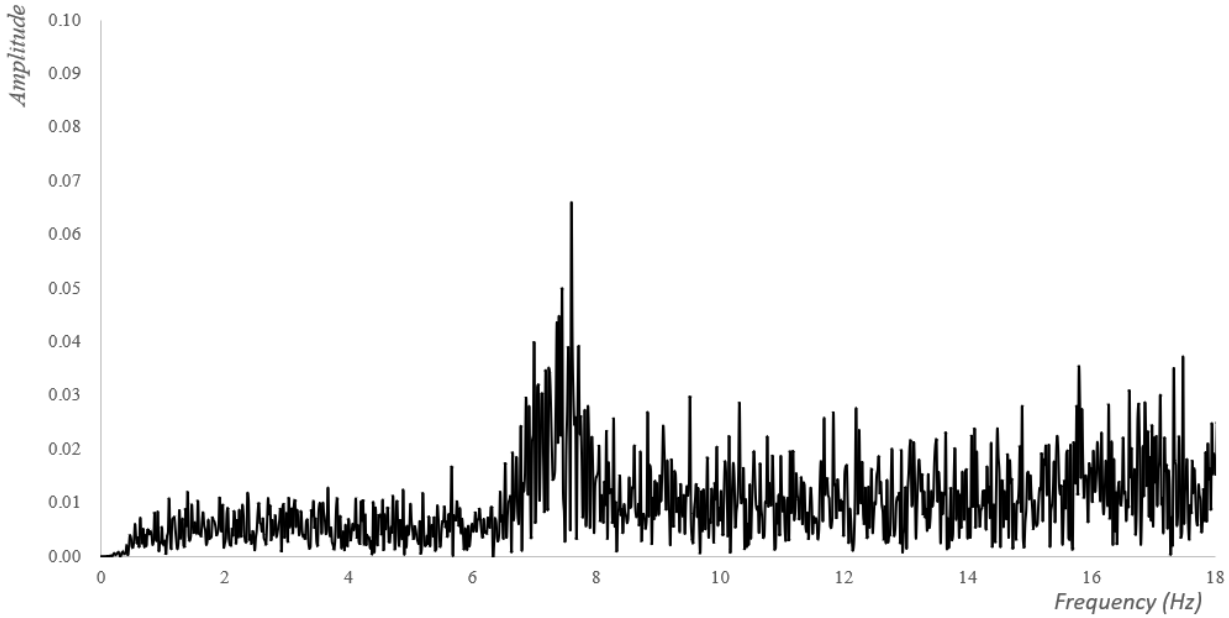

Figure 1.5 Single-sided amplitude spectrum (pre-amplification at the natural frequency of SDOF structure)

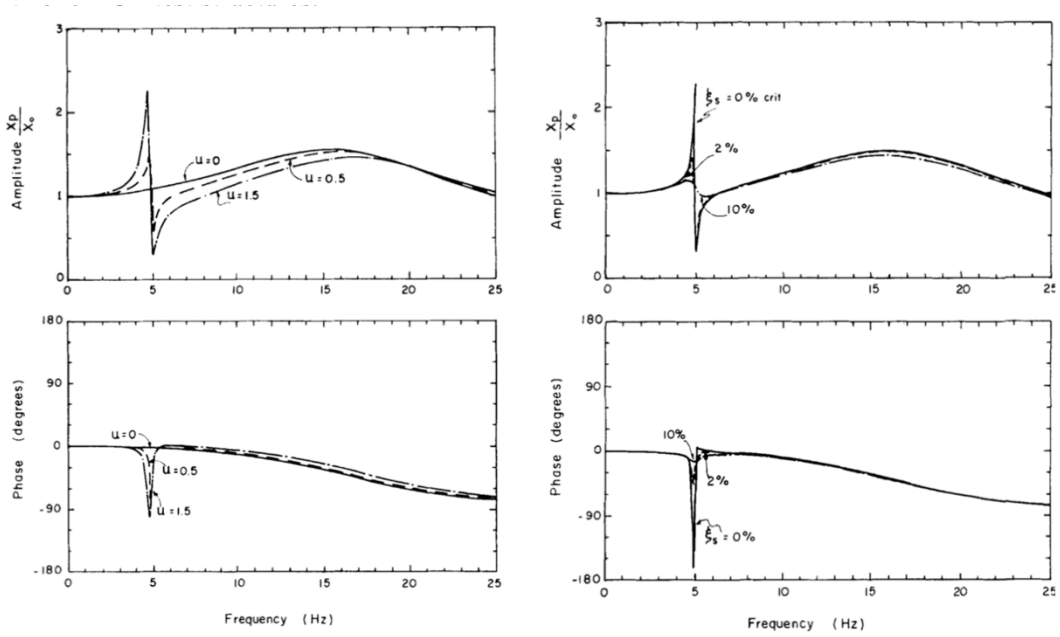

Figure 2.1 Effect of structure properties on frequency response of SDOF system (structural mass ratio in left figure and structure's damping in right figure)

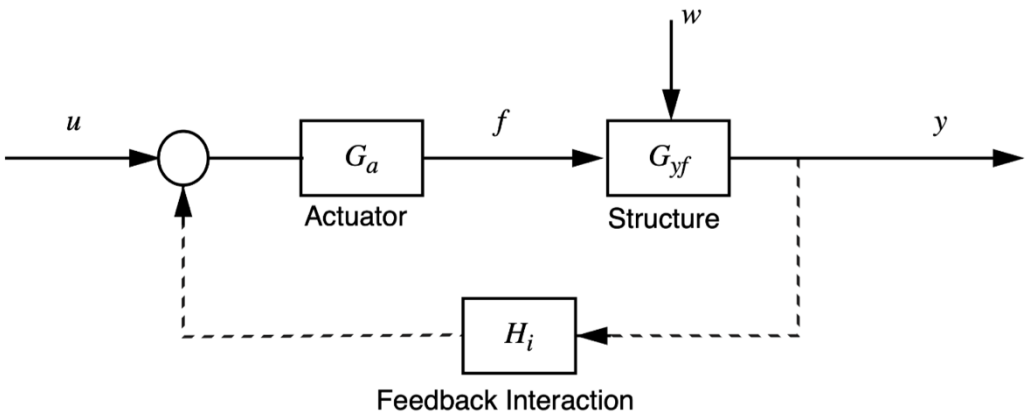

Figure 2.2 Model of interaction between the actuator and the structure

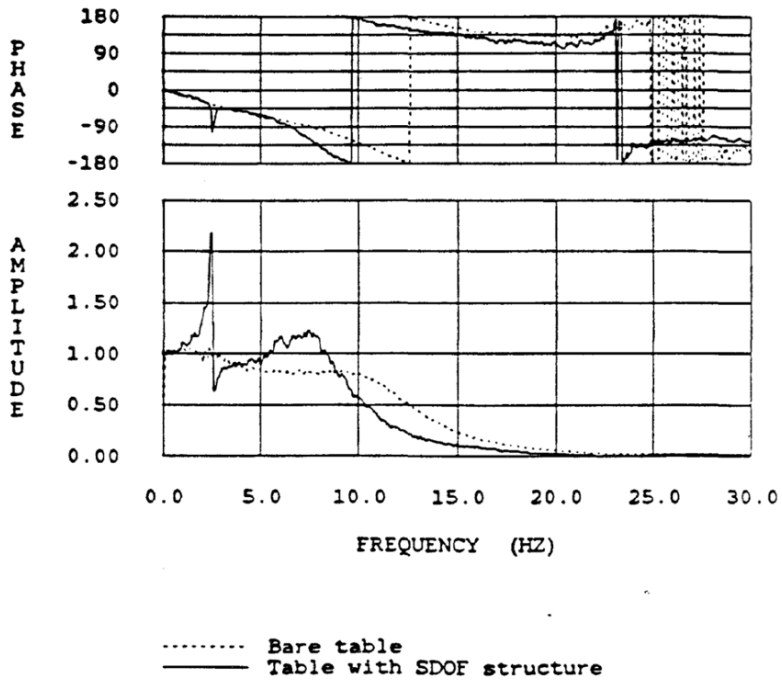

Figure 2.3 Transfer functions of table horizontal displacement over horizontal command displacement

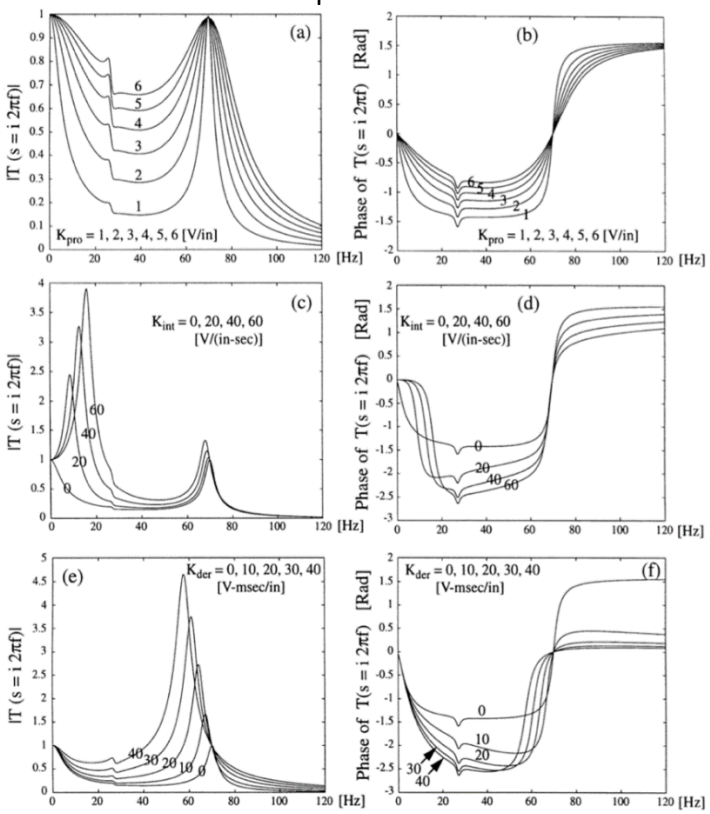

Figure 2.4 Effects of the PID control gains upon the shaking table transfer function for bare table condition

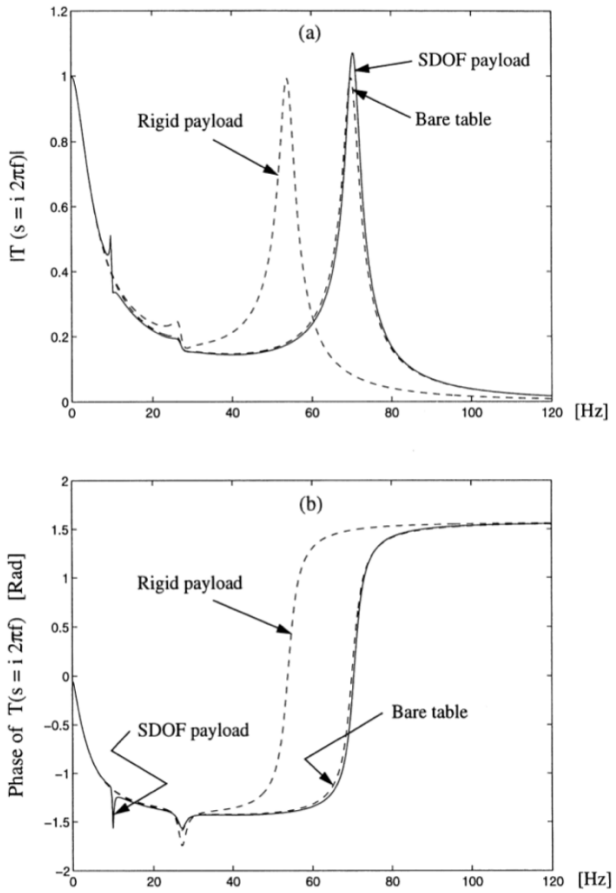

Figure 2.5 (a) Magnitude and (b) phase of table transfer function (including base flexibility) for (i) bare table condition, (ii) table loaded with a 408 kg (900 lbs) rigid payload, and (iii) table loaded with a 408 kg (900 lbs) SDOF payload

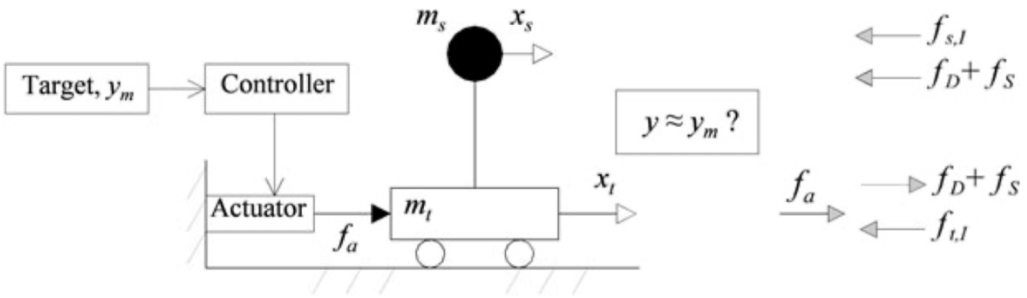

Figure 2.6 Schematic of a shake table-structure system

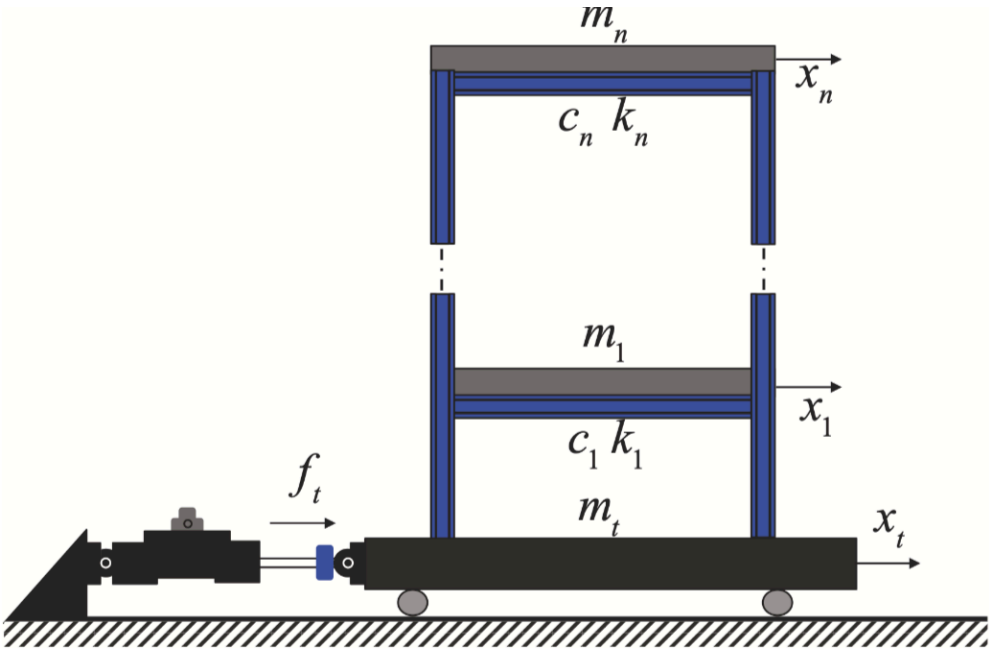

Figure 2.7 Schematic of a uni-axial shake table with linear structure

Table 3.1: Parameters of EERC's and NBUT's Numerical Model

Parameters (units)	Signals	EERC	NBUT
Structural Mass $(\boldsymbol{kips - sec^2/in})$	$\boldsymbol{Mst}$	0.1771	0.0372
Structural Stiffness $(\boldsymbol{kips/in})$	$\boldsymbol{Kst}$	57.9	71.96
Structural Damping $(\boldsymbol{kips - sec^2/in})$	$\boldsymbol{Cst}$	0.128	0.0655
Table Mass $(\boldsymbol{kips - sec^2/in})$	$\boldsymbol{Mt}$	0.2588	0.0885
Time Delay (s)	$\boldsymbol{T_d}$	0.015	0.001
Table Horizontal Damping $(\boldsymbol{kips - sec^2/in})$	$\boldsymbol{Ct}$	6.126	6
Main-stage Value Null Flow Gain $(\boldsymbol{in^3/sec/\%})$	$\boldsymbol{K_v}$	1894.6	1361.4
Compressibility Coefficient $(\boldsymbol{in^3/ksi})$	$\boldsymbol{K_a}$	1.191	1
Leakage Flow $(\boldsymbol{in^3 - ksi/sec})$	$\boldsymbol{Cl}$	23	7
Piston Area $(\boldsymbol{in^2})$	$\boldsymbol{A}$	25.4	10

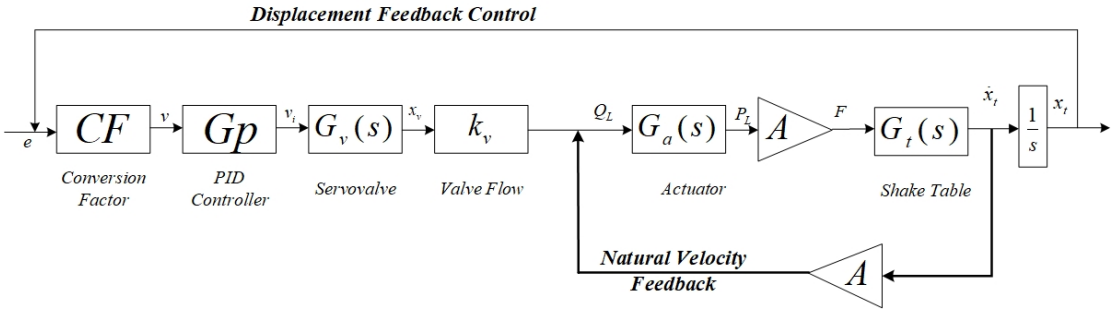

Figure 3.1 Block diagram of bare table system with displacement feedback control

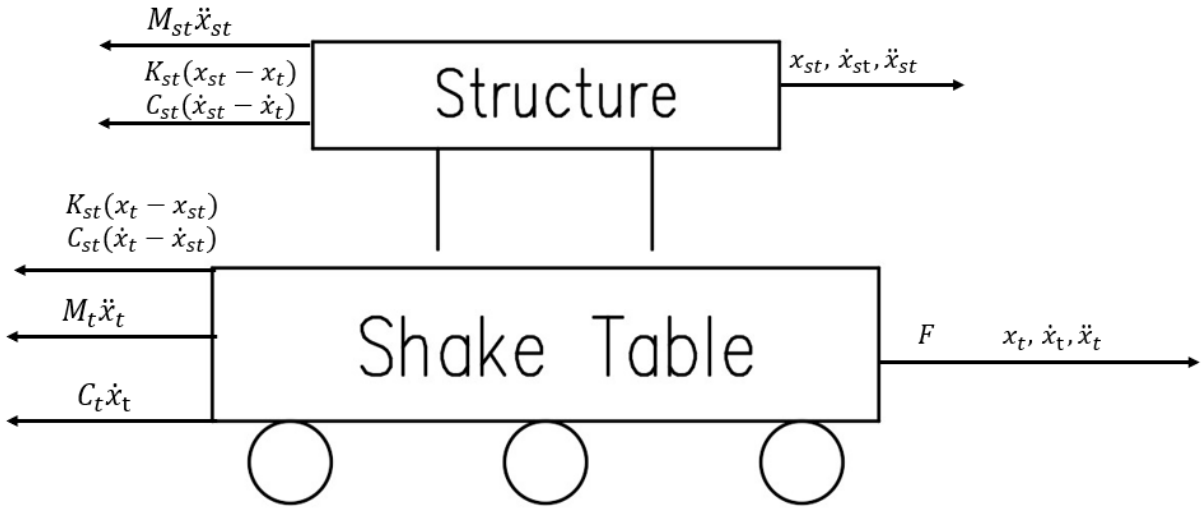

Figure 3.2 Free body diagrams of shake table and test structure

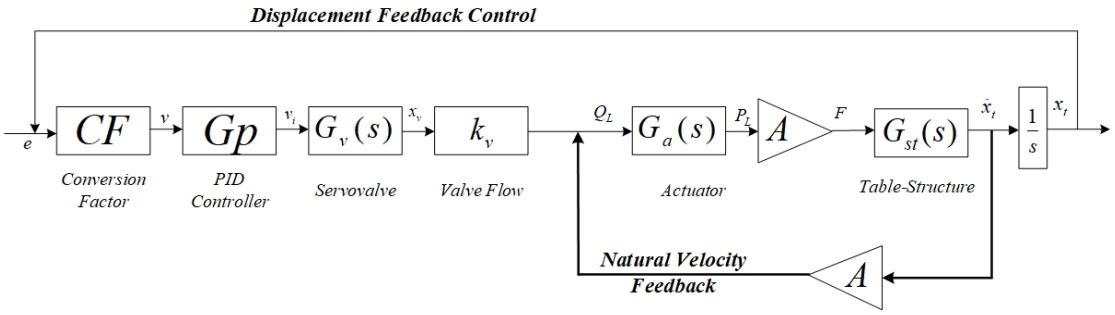

Figure 3.3 Block diagram of table-structure system with displacement feedback control

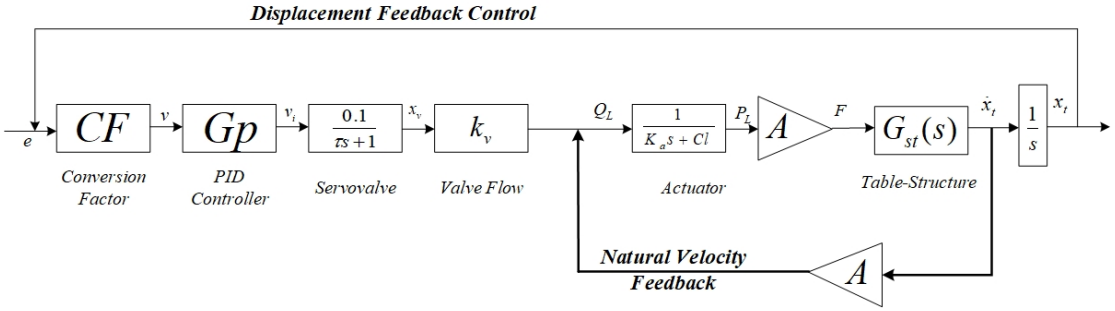

Figure 3.4 Detailed transfer functions for table-structure system

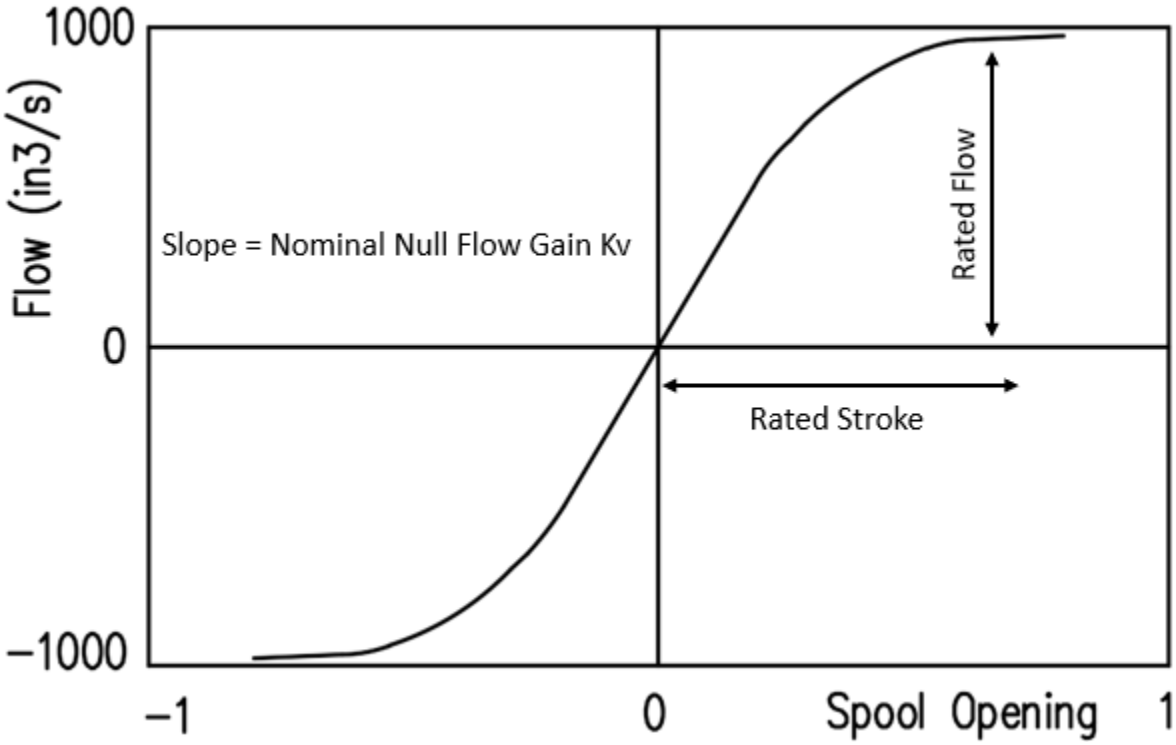

Figure 3.5 Nonlinear Flow Model

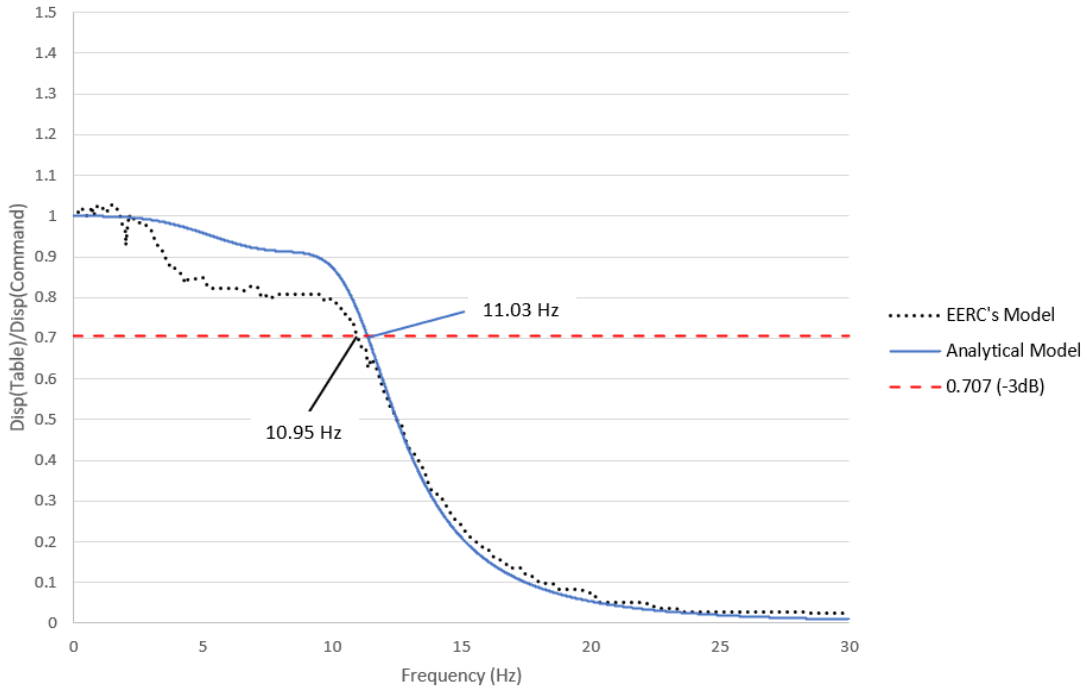

Figure 4.1 Comparison for transfer functions between analytical model and EERC's for bare table

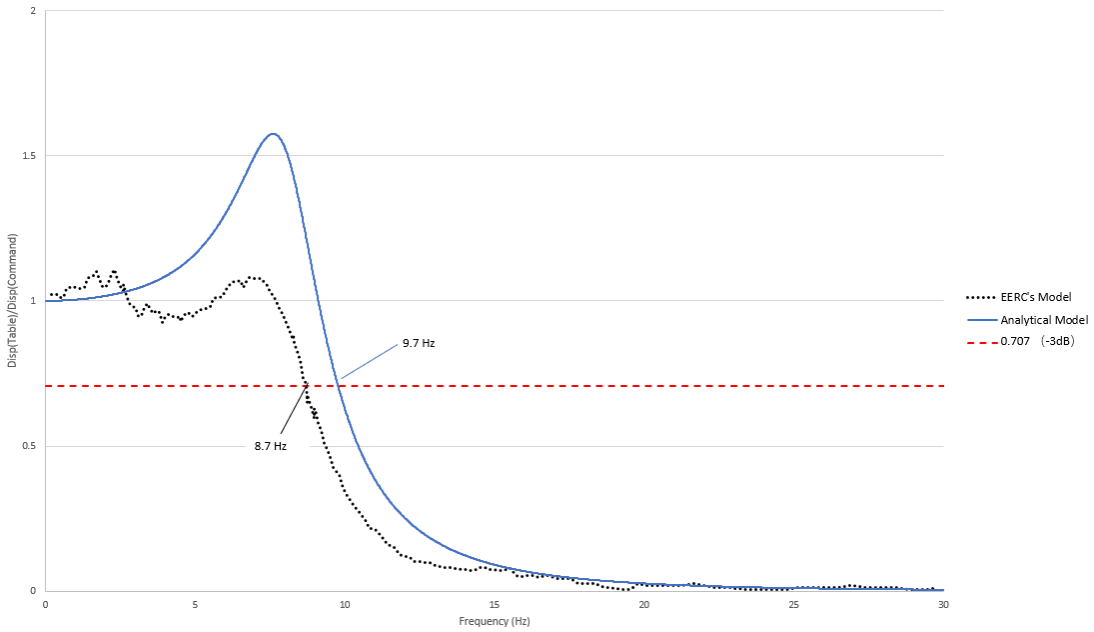

Figure 4.2 Comparison for transfer functions between analytical model and EERC's for table loaded with 70 kips mass

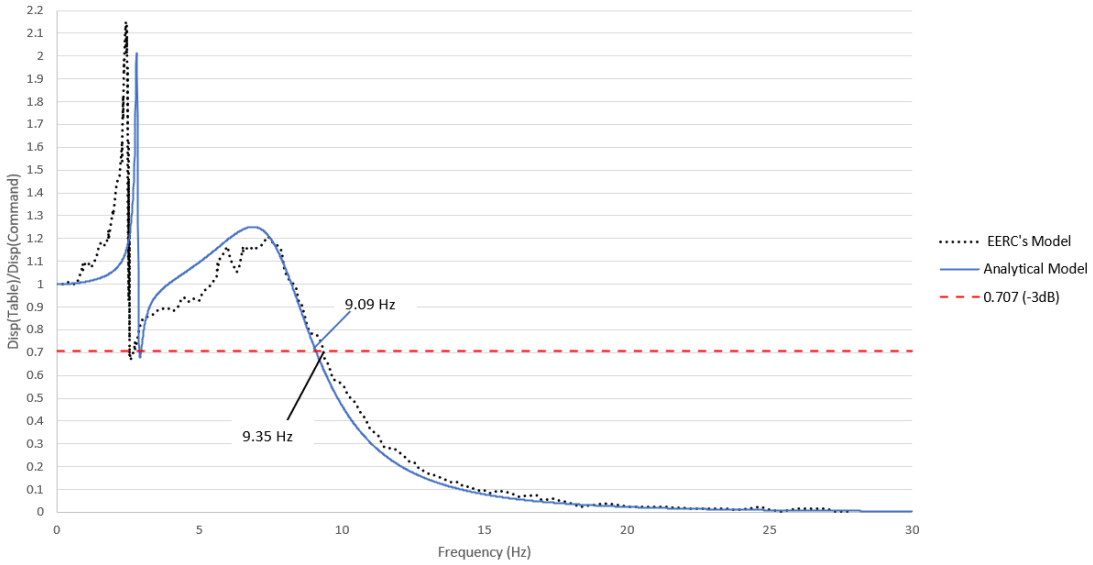

Figure 4.3 Comparison for transfer functions between analytical model and EERC's for table loaded with SDOF structure

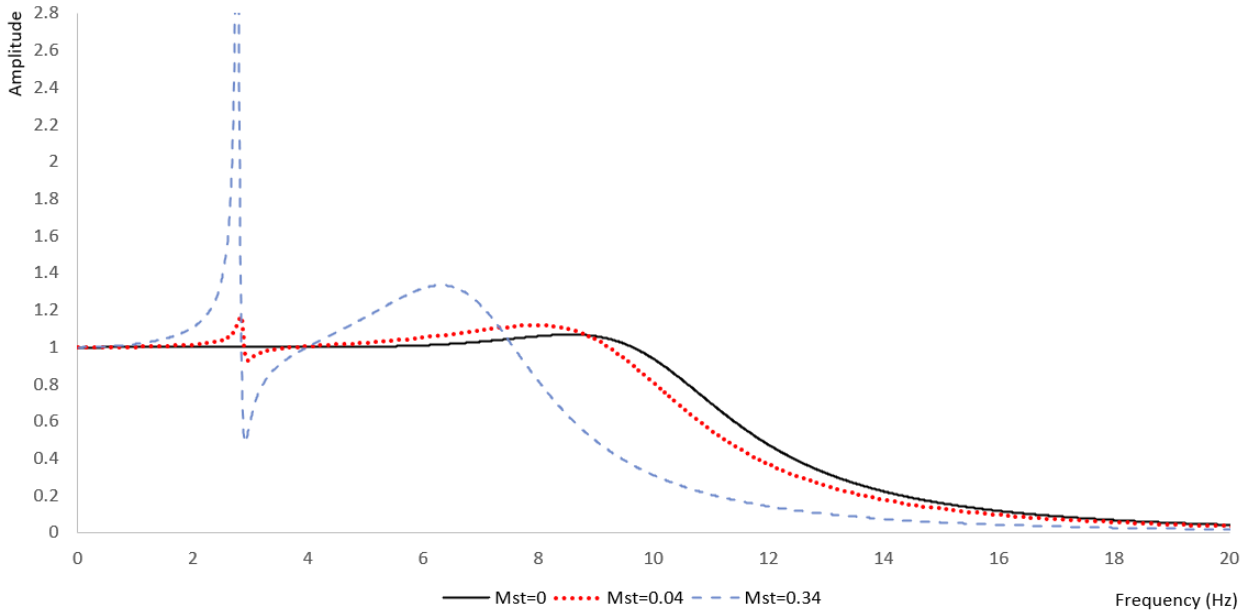

Figure4.4 Effects of changing structural mass for displacement feedback system

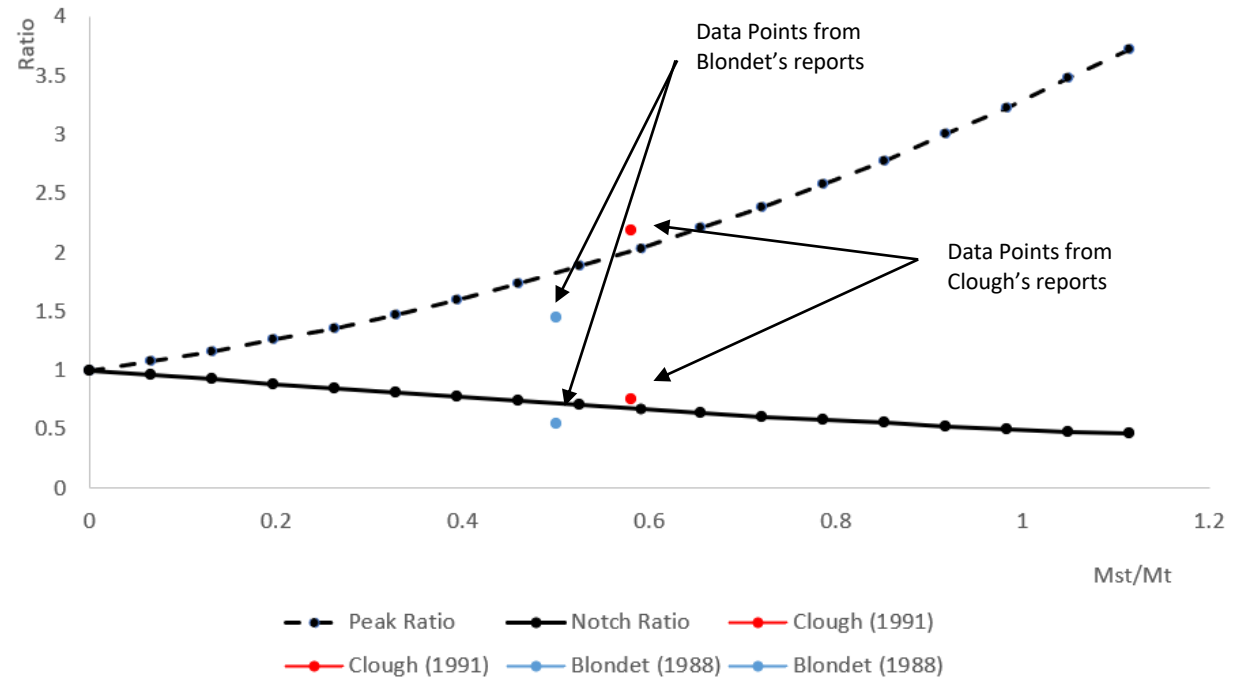

Figure 4.5 Effects of changing structural mass on peak and notch value

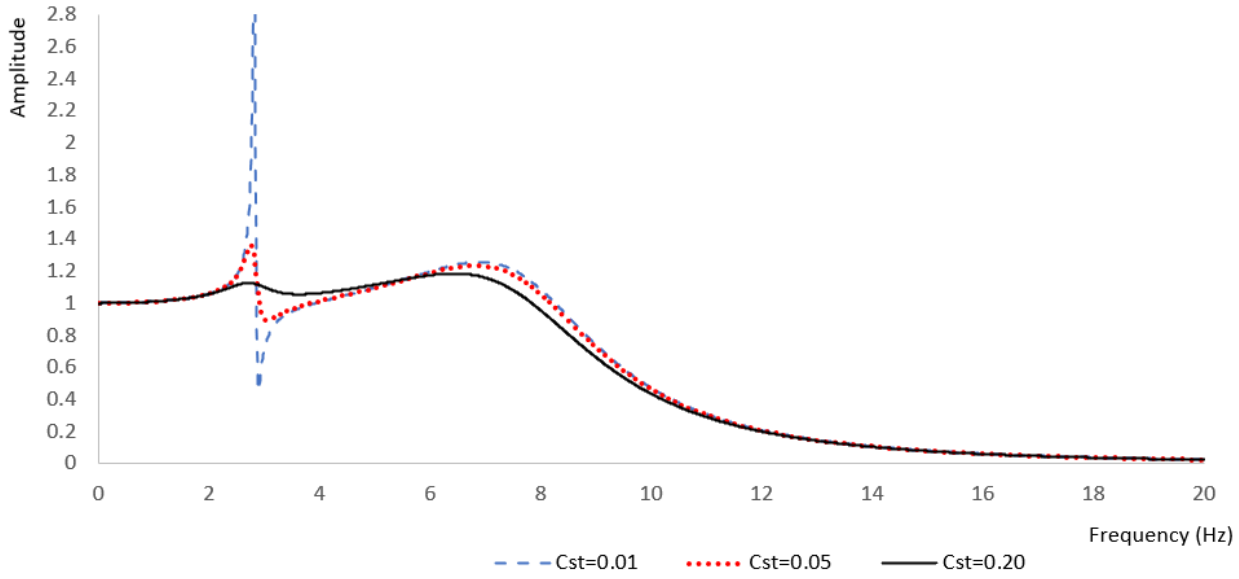

Figure 4.6 Effects of changing structural damping for displacement feedback system

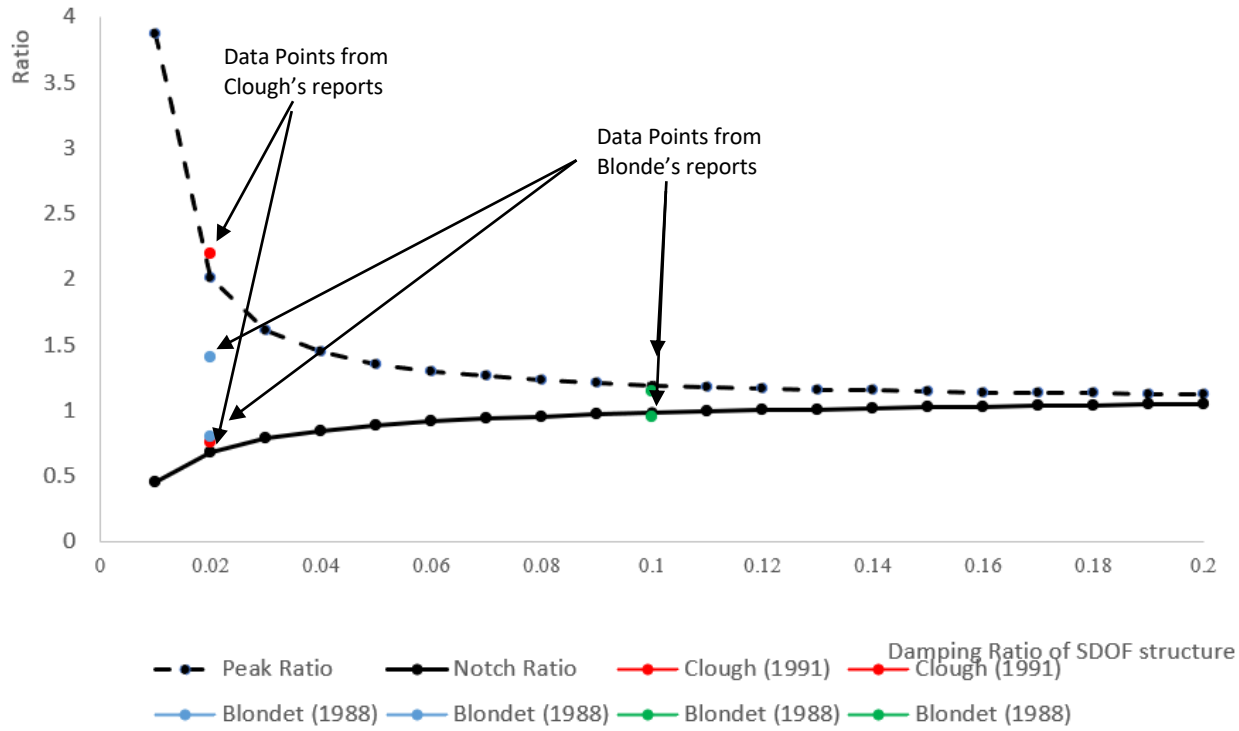

Figure 4.7 Effects of changing structural damping on peak and notch value

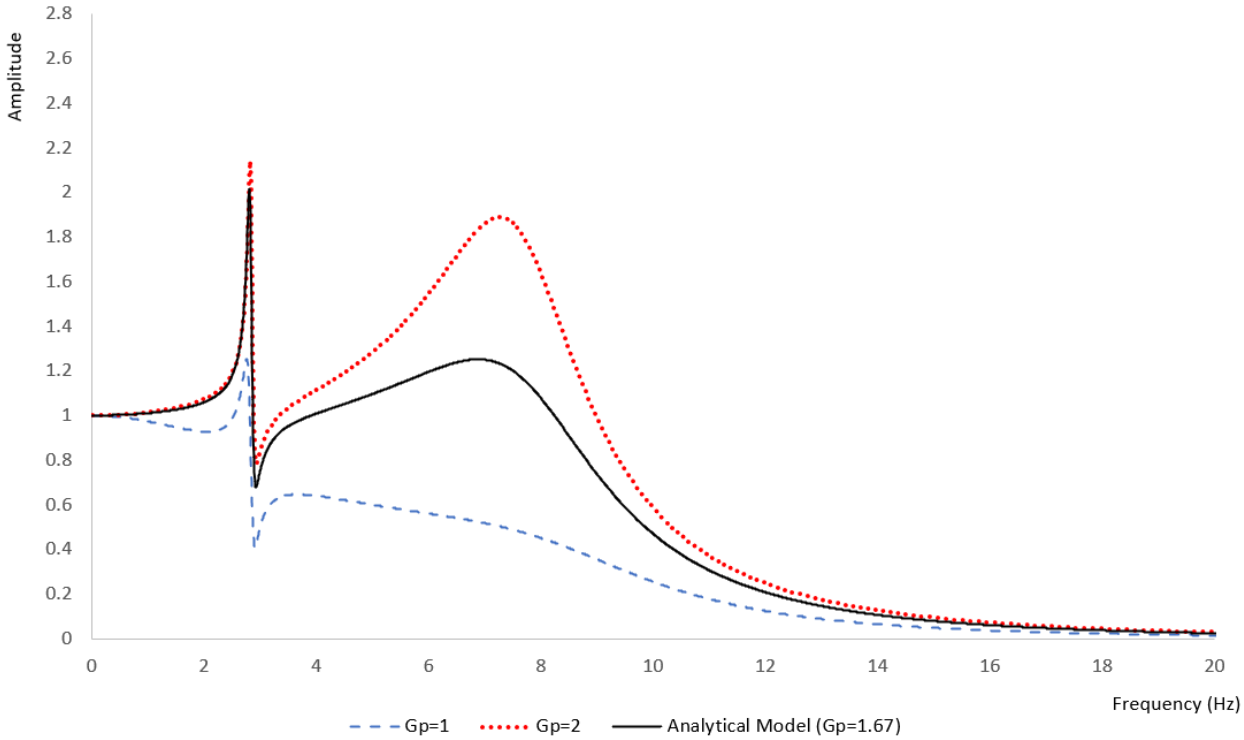

Figure 4.8 Effects of changing Proportional gain for displacement feedback system

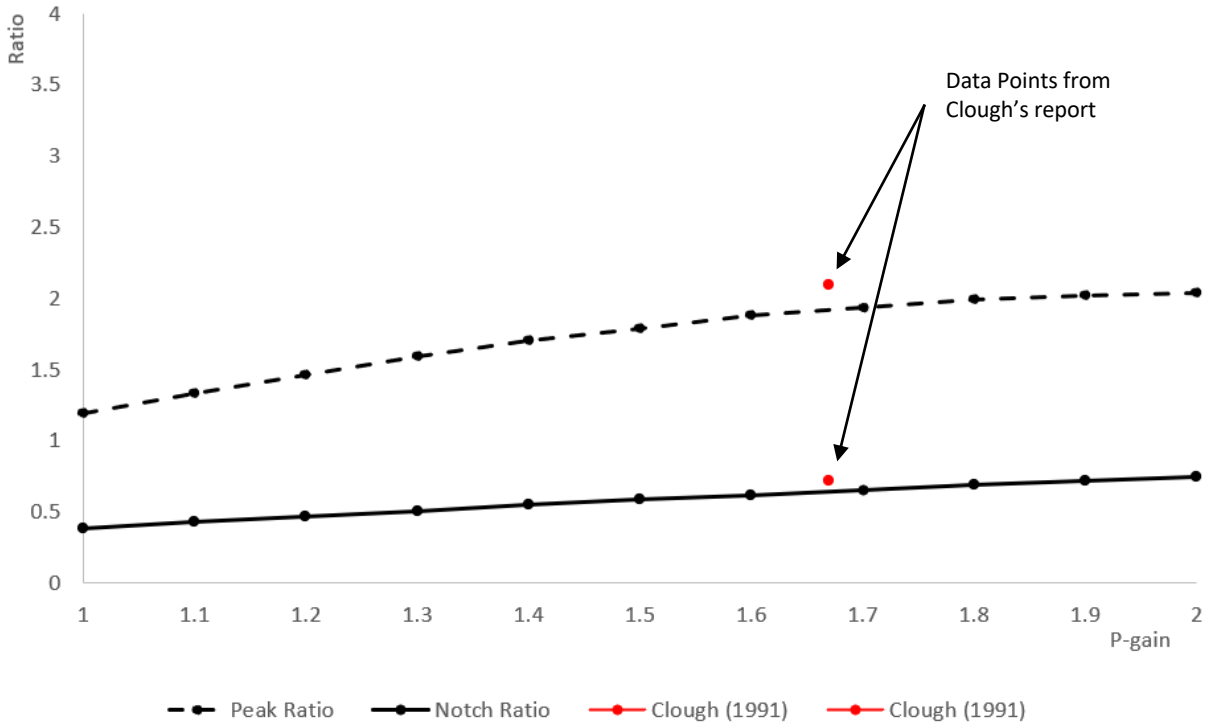

Figure 4.9 Effects of changing Proportional gain on peak and notch value

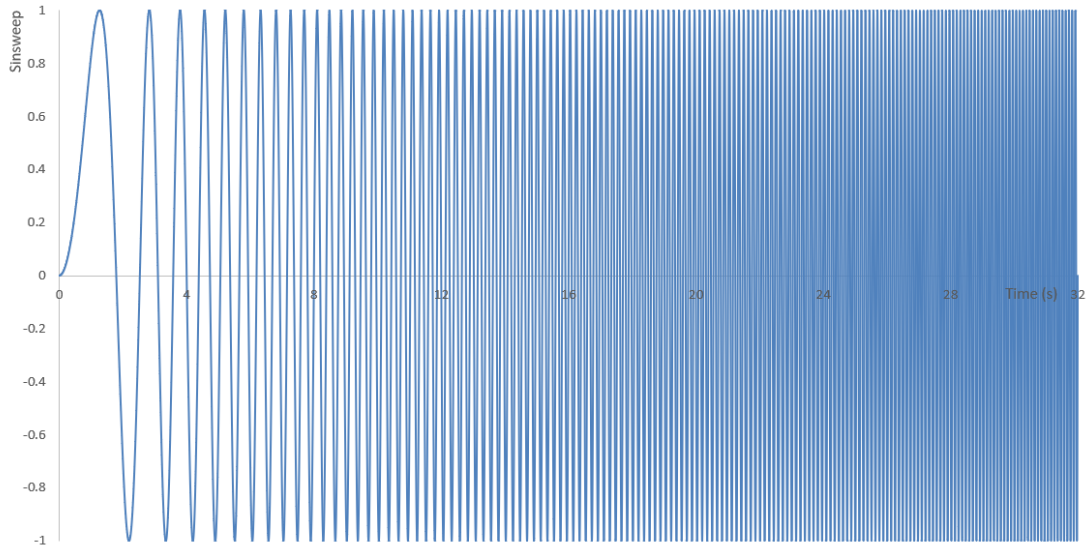

Figure5.1 Sin sweep reference

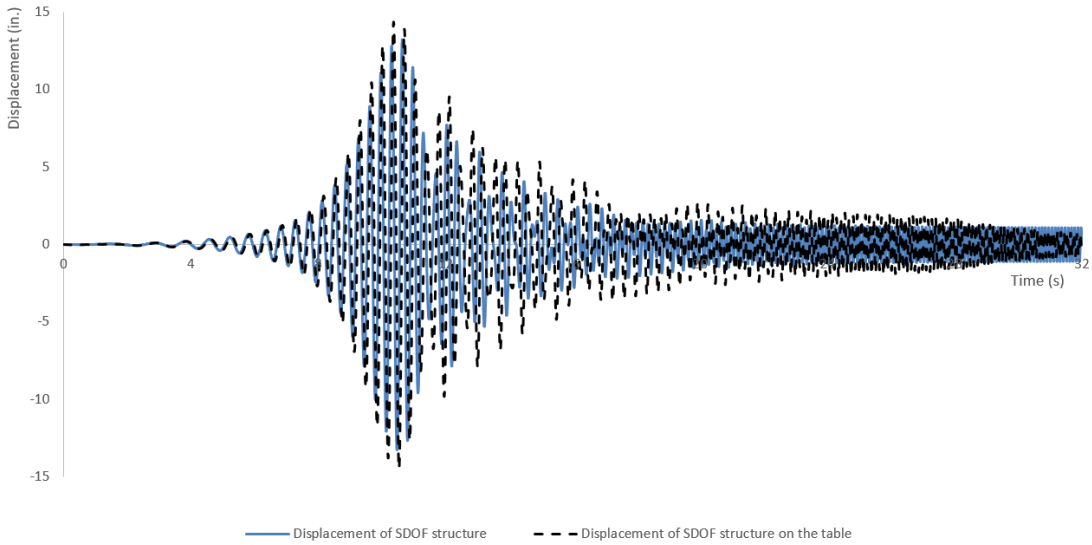

Figure 5.2 Comparison for displacement between structure on the ground and structure (2.87 Hz) on the table in time domain for EERC's table (Sin sweep)

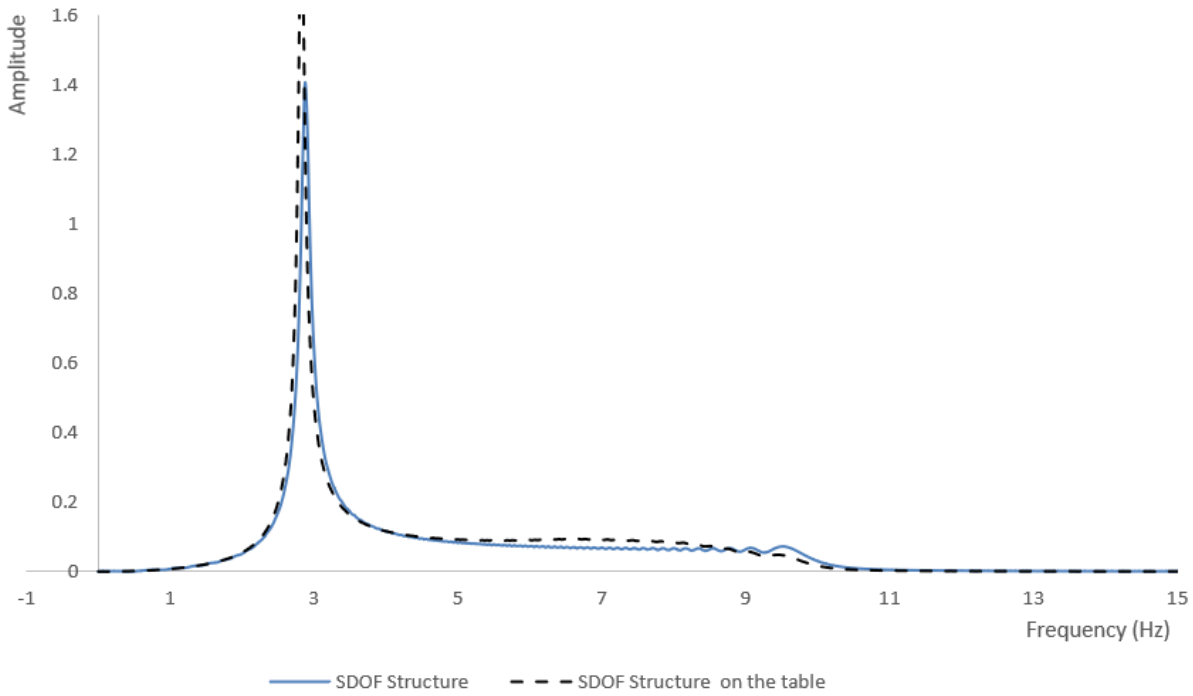

Figure 5.3 FFT response of SDOF structural displacement on the ground and SDOF structural (2.87 Hz) relative displacement mounted on the table for EERC's table (Sin sweep)

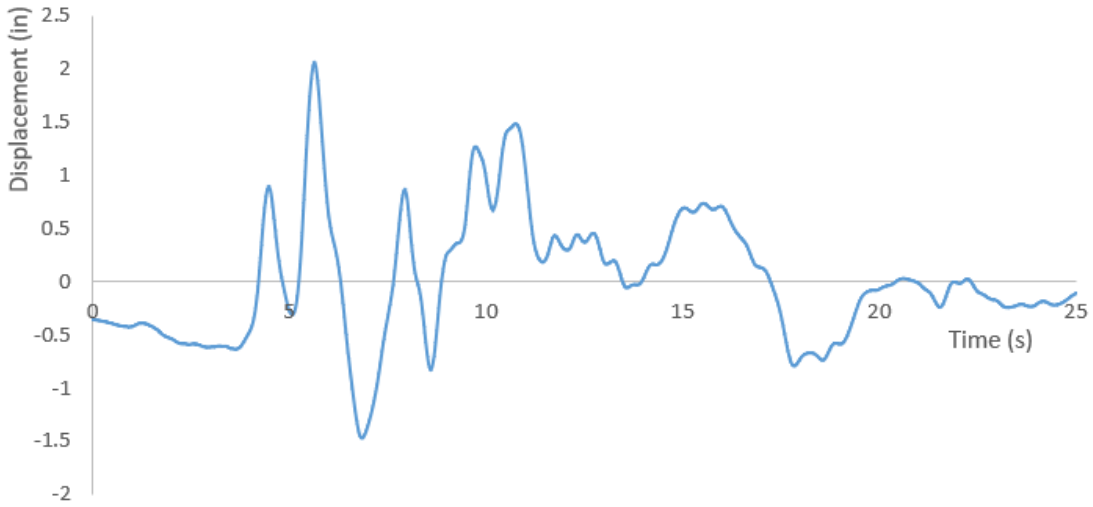

Figure 5.4 Kobe Earthquake

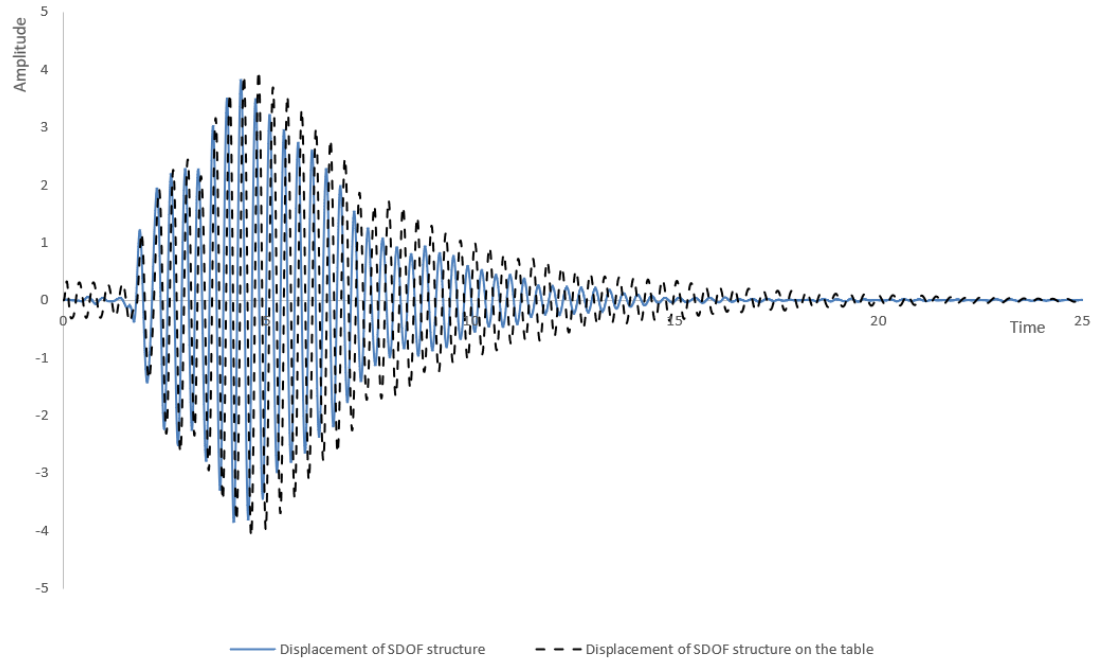

Figure 5.5 Comparison for displacement between structure on the ground and structure (2.87 Hz) on the table in time domain for EERC's table (Kobe)

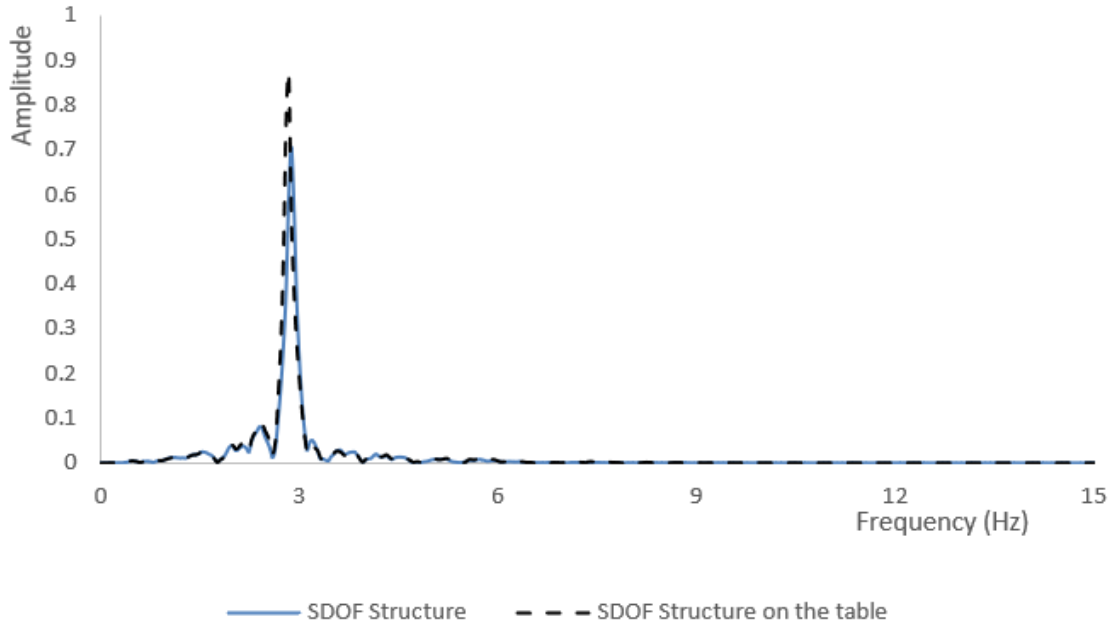

Figure 5.6 FFT response of SDOF structural displacement on the ground and SDOF structure's (2.87 Hz) relative displacement mounted on the table for EERC's table (Kobe)

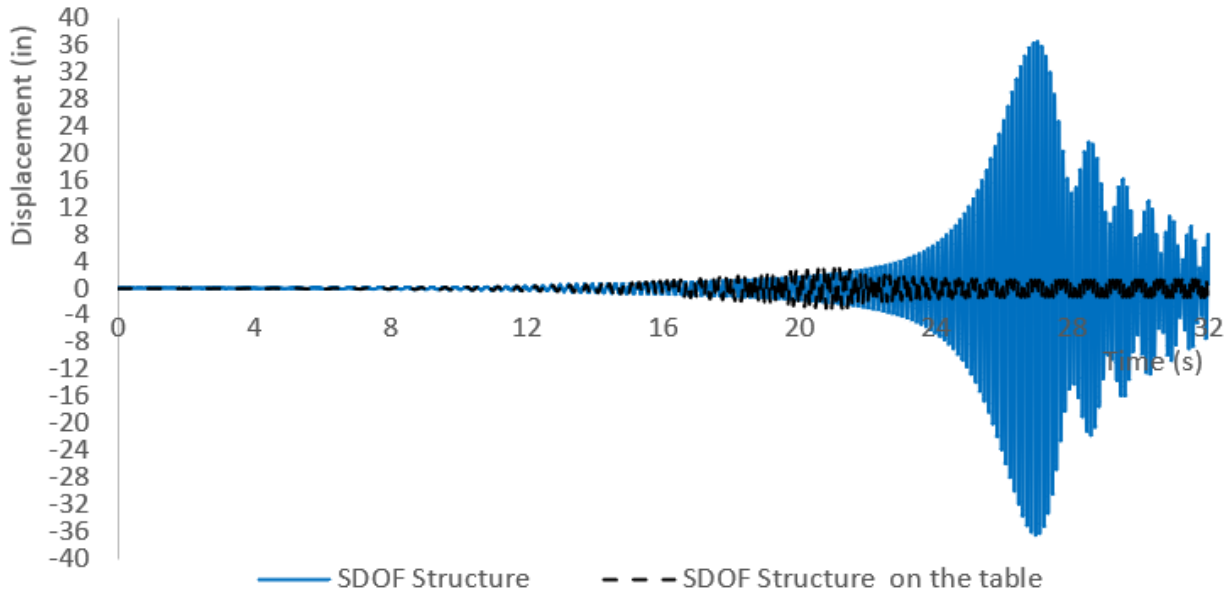

Figure 5.7 Comparison for displacement between structure on the ground and structure (8 Hz) on the table in time domain for EERC's table (Sin sweep)

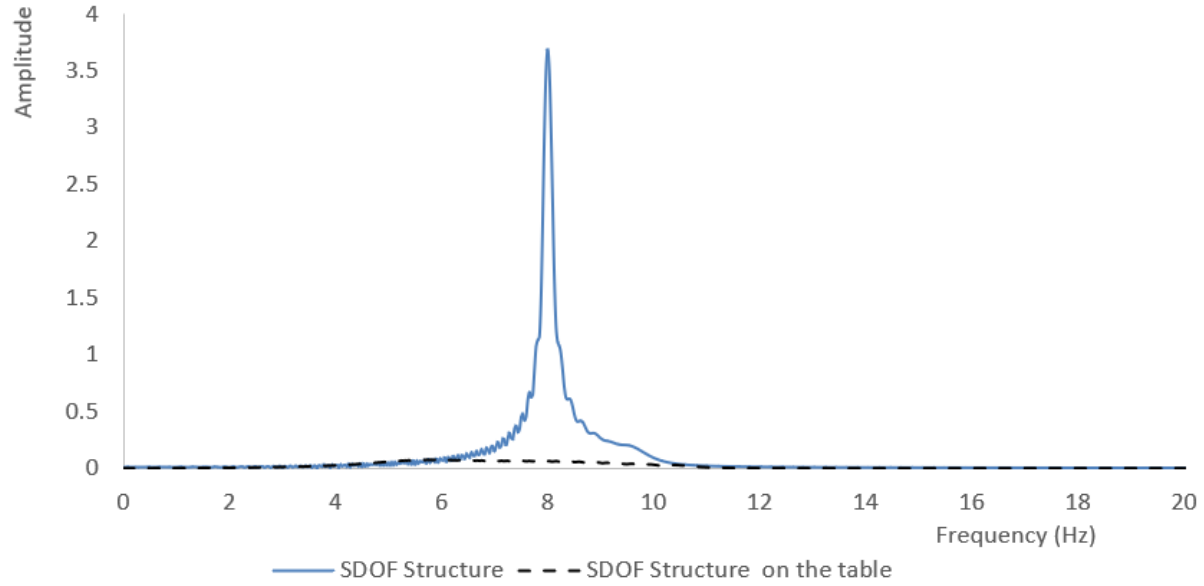

Figure 5.8 FFT response of SDOF structural displacement on the ground and SDOF structure's (8 Hz) relative displacement mounted on the table for EERC's table (Sin sweep)

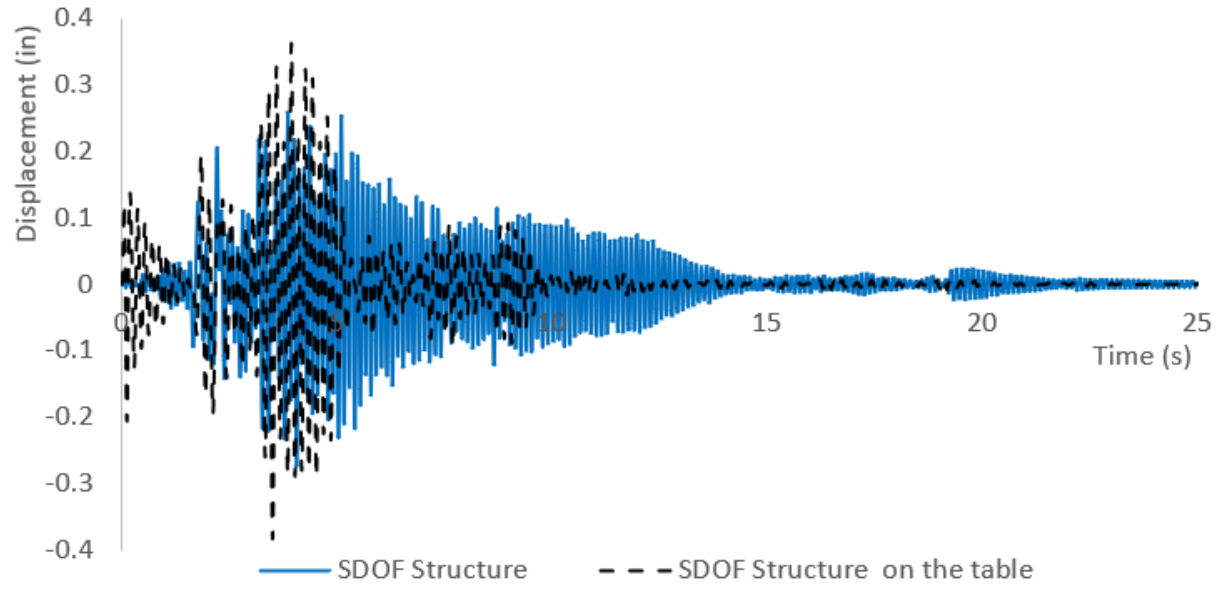

Figure 5.9 Comparison for displacement between structure on the ground and structure (8 Hz) on the table in time domain for EERC's table (Kobe)

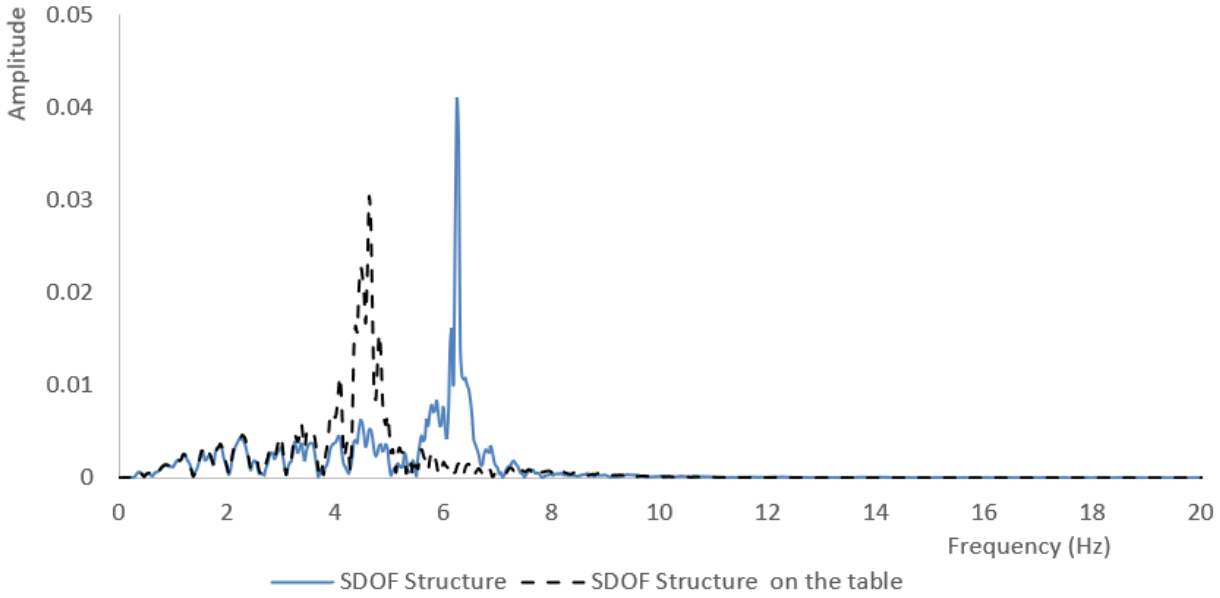

Figure 5.10 Comparison for displacement between structure on the ground and structure (8 Hz) on the table in frequency domain for EERC's table (Kobe)

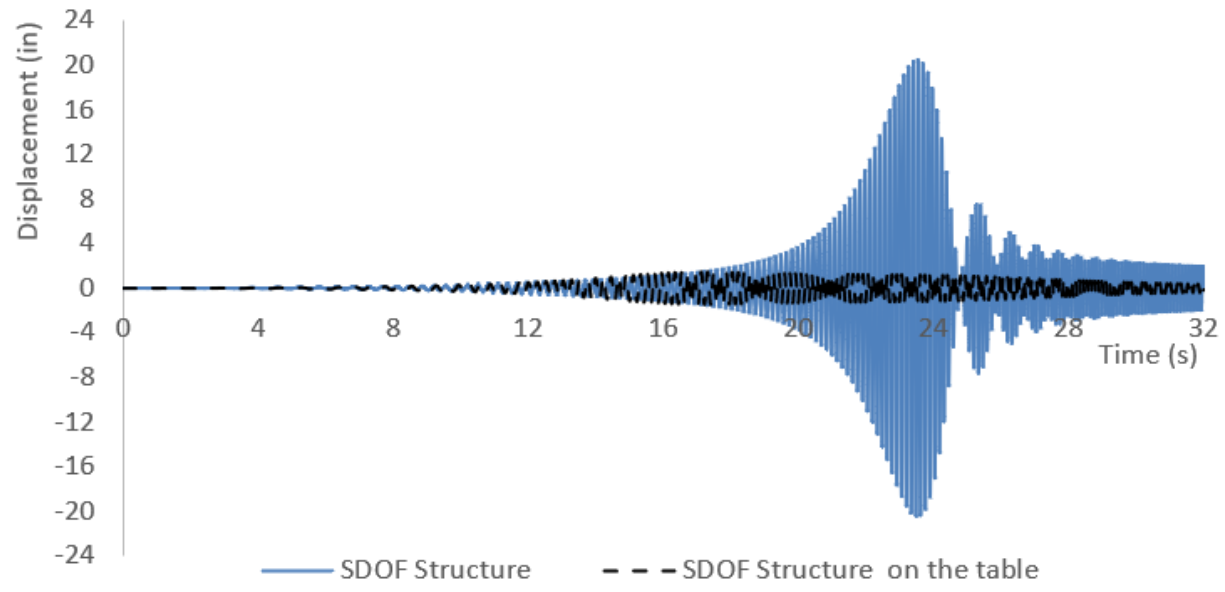

Figure 5.11 Comparison for displacement between structure on the ground and structure (7Hz) on the table in time domain for NBUT's table (Sin sweep)

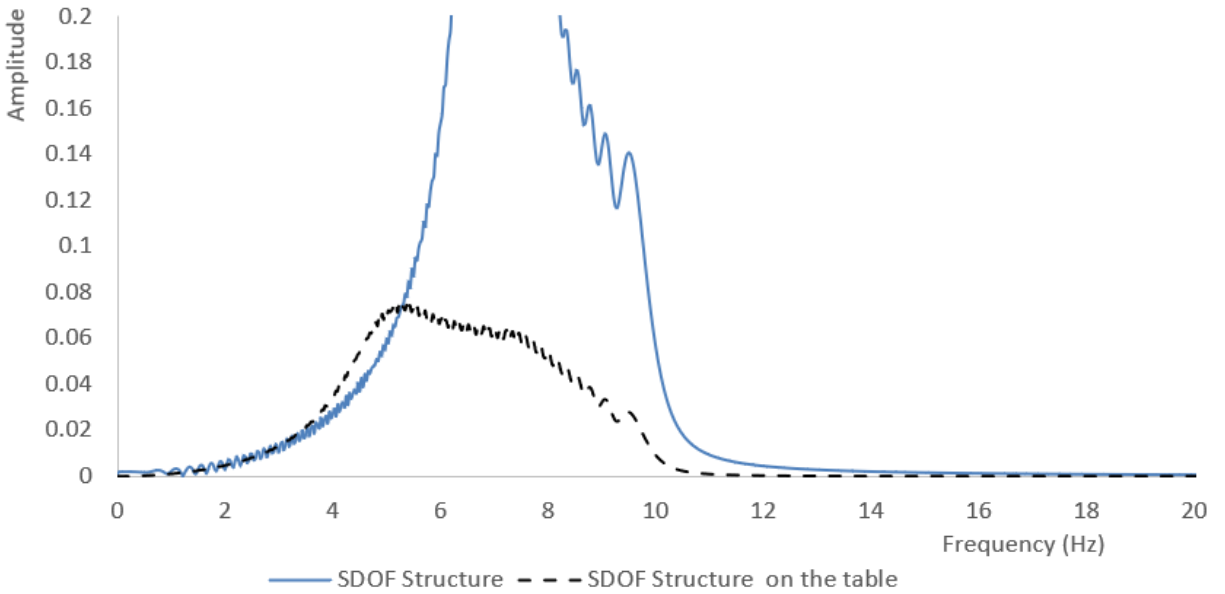

Figure 5.12 FFT response of SDOF structural displacement on the ground and SDOF structure's (7Hz) relative displacement mounted on the table for NBUT's table (Sin sweep)

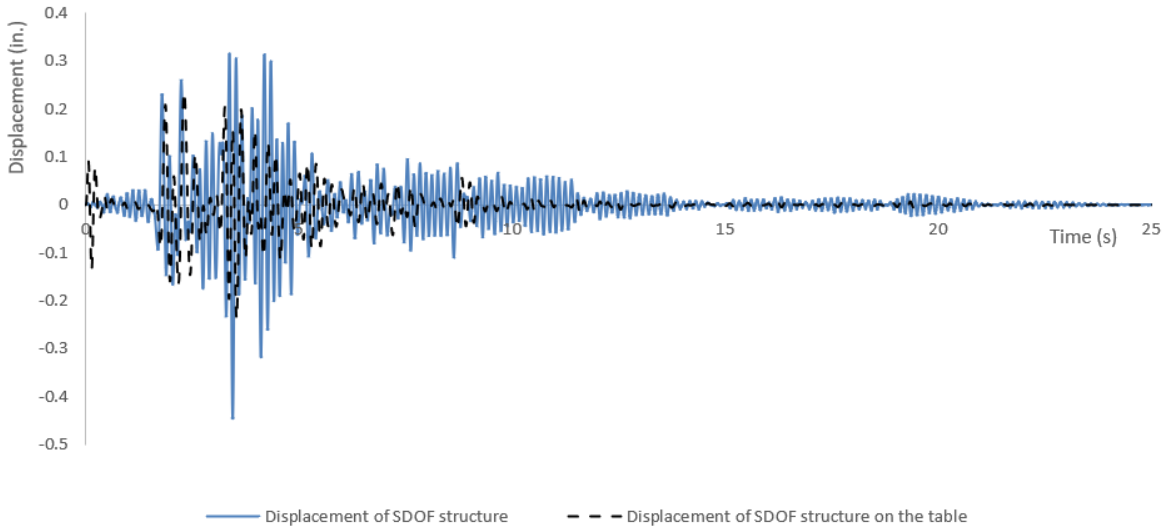

Figure 5.13 Comparison for displacement between structure on the ground and structure (7Hz) on the table in time domain for NBUT's table (Kobe)

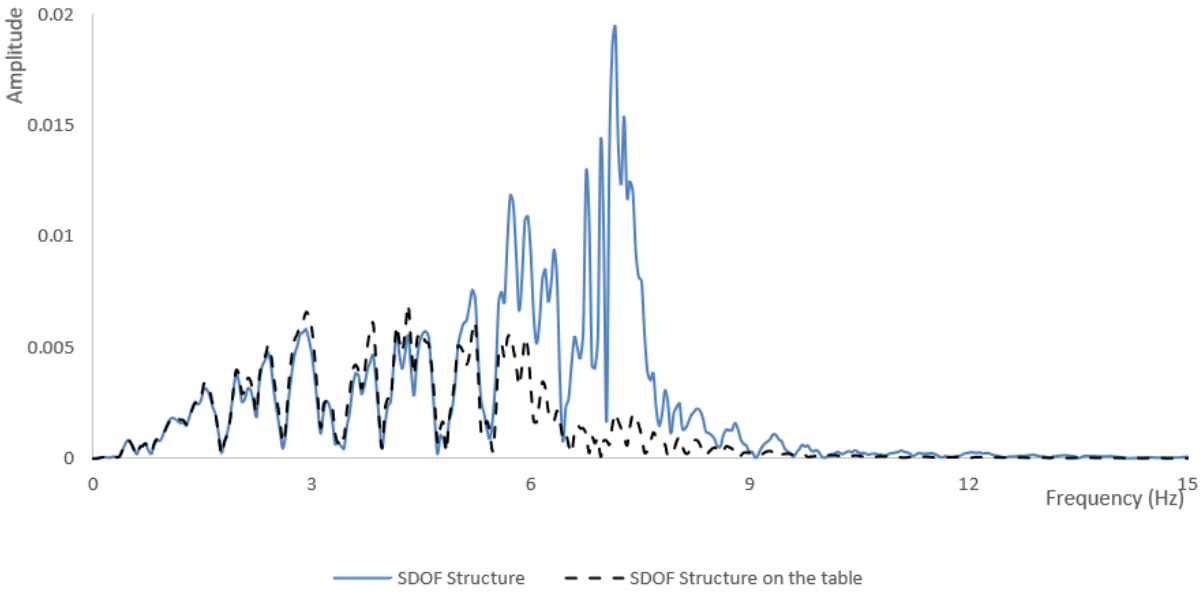

Figure 5.14 FFT response of SDOF structural displacement on the ground and SDOF structure's (7Hz) relative displacement mounted on the table for NBUT's table (Kobe)

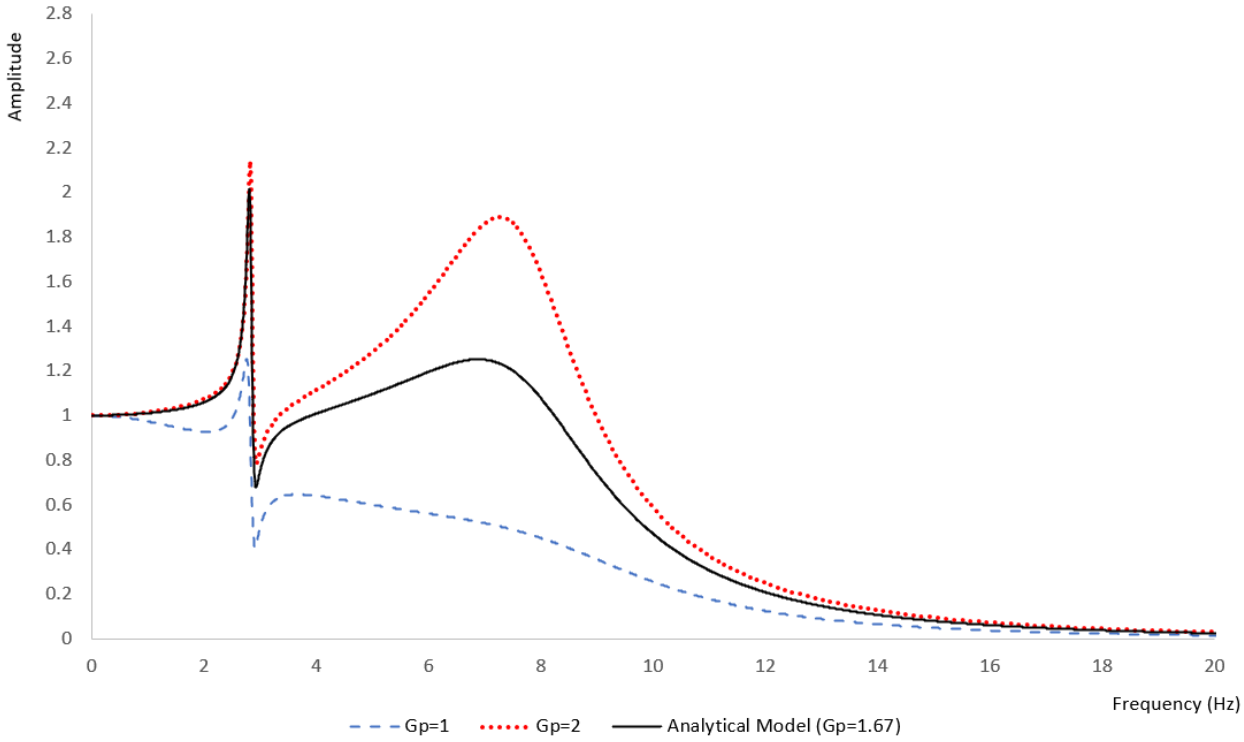

Figure 5.15 Effects of changing Proportional gain for EERC's shake table system

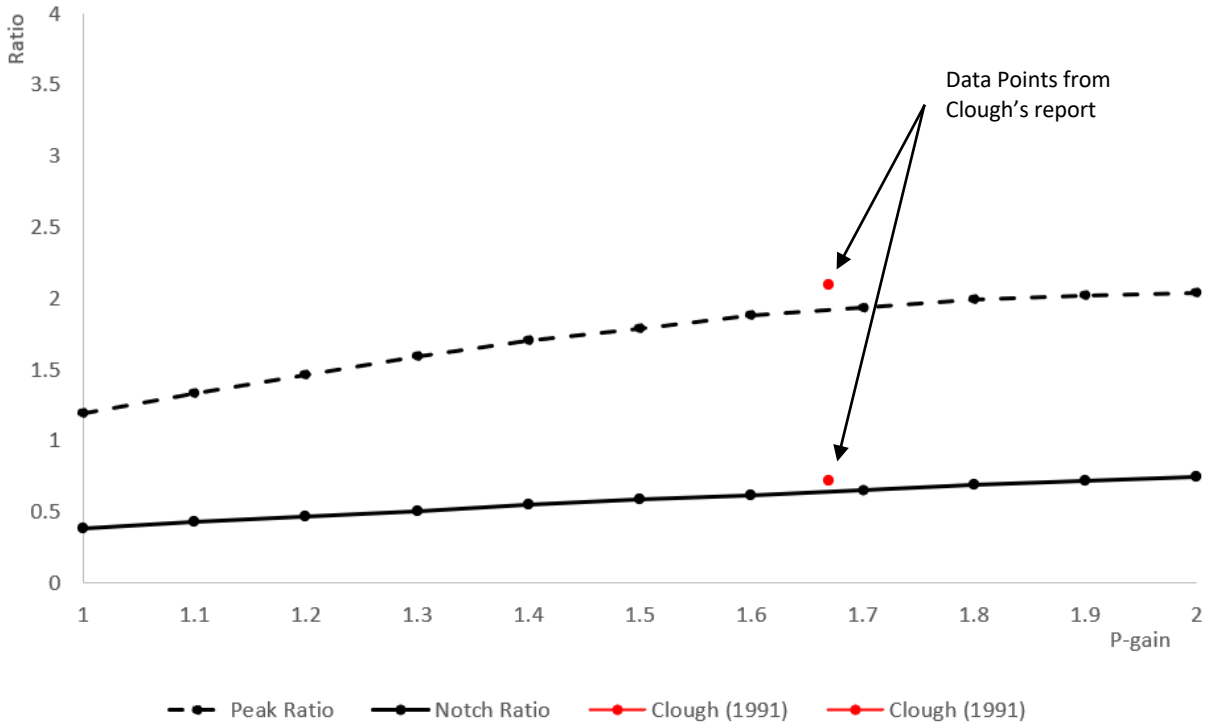

Figure 5.16 Effects of changing Proportional gain on peak and notch value for EERC's shake table system

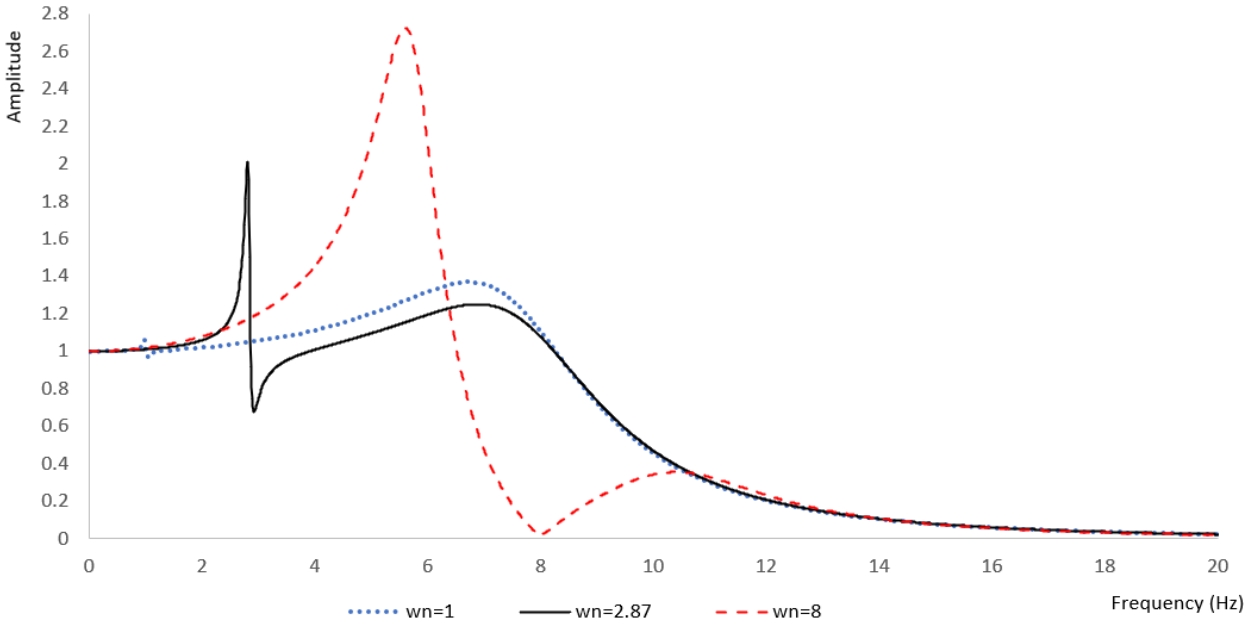

Figure 5.17 Effects of changing structural frequency for EERC's shake table system

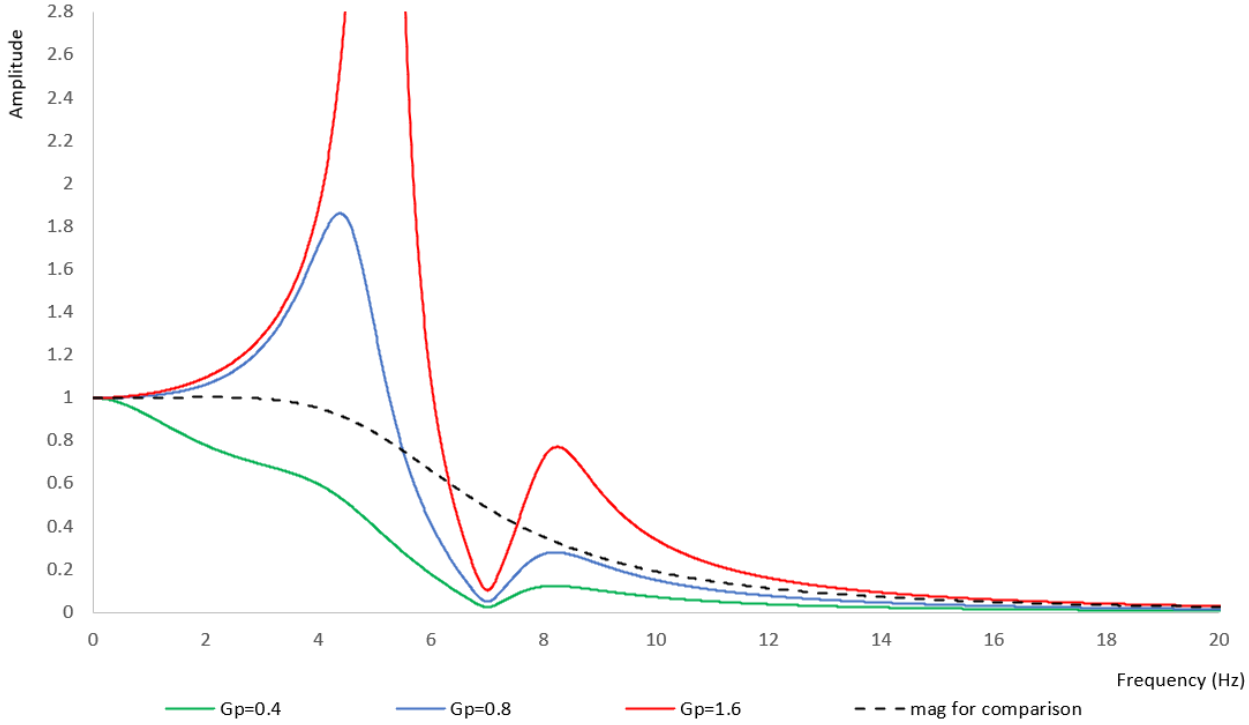

Figure 5.18 Effects of changing proportional gain for NBUT's model loaded with 7 Hz SDOF structure

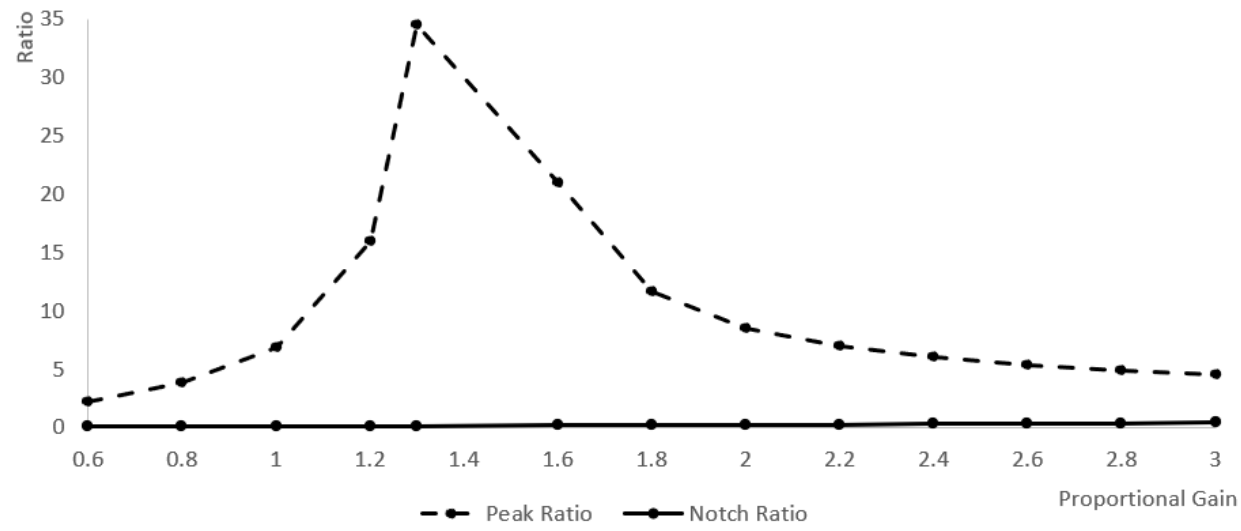

Figure 5.19 Effects of changing Proportional gain on peak and notch value for NBUT's model loaded with 7 Hz SDOF structure

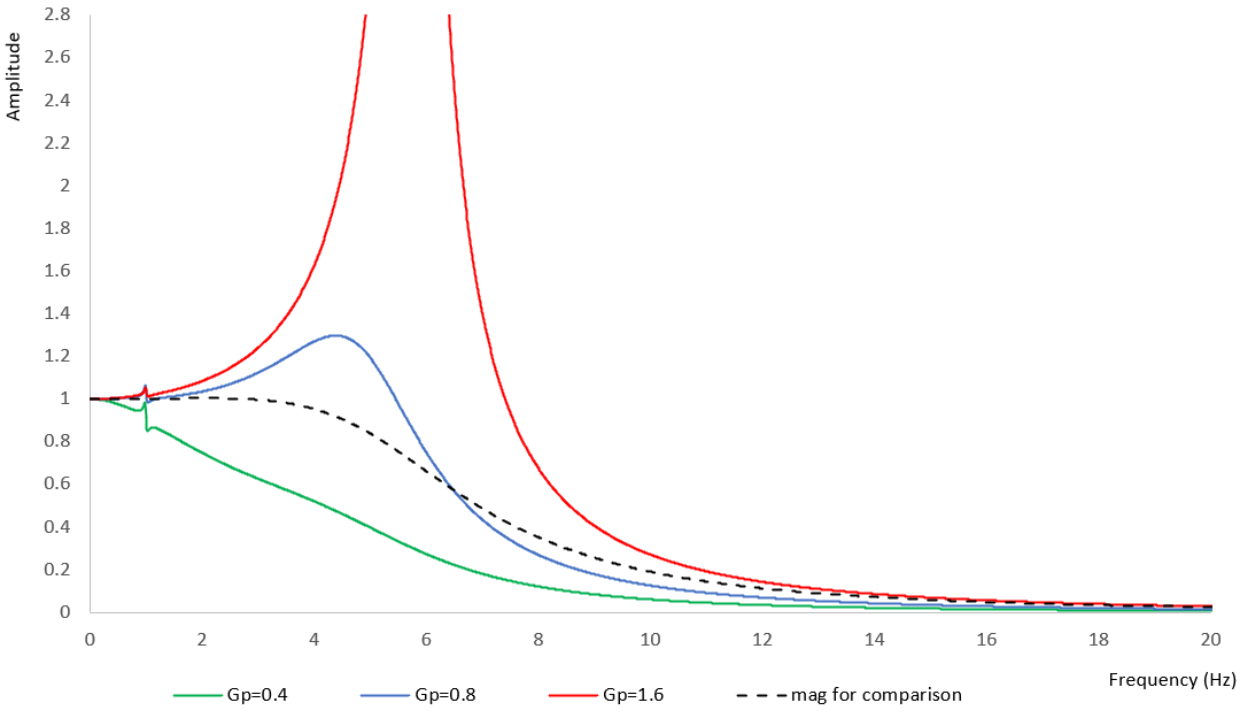

Figure 5.20 Effects of changing proportional gain for NBUT's model loaded with 1 Hz SDOF structure

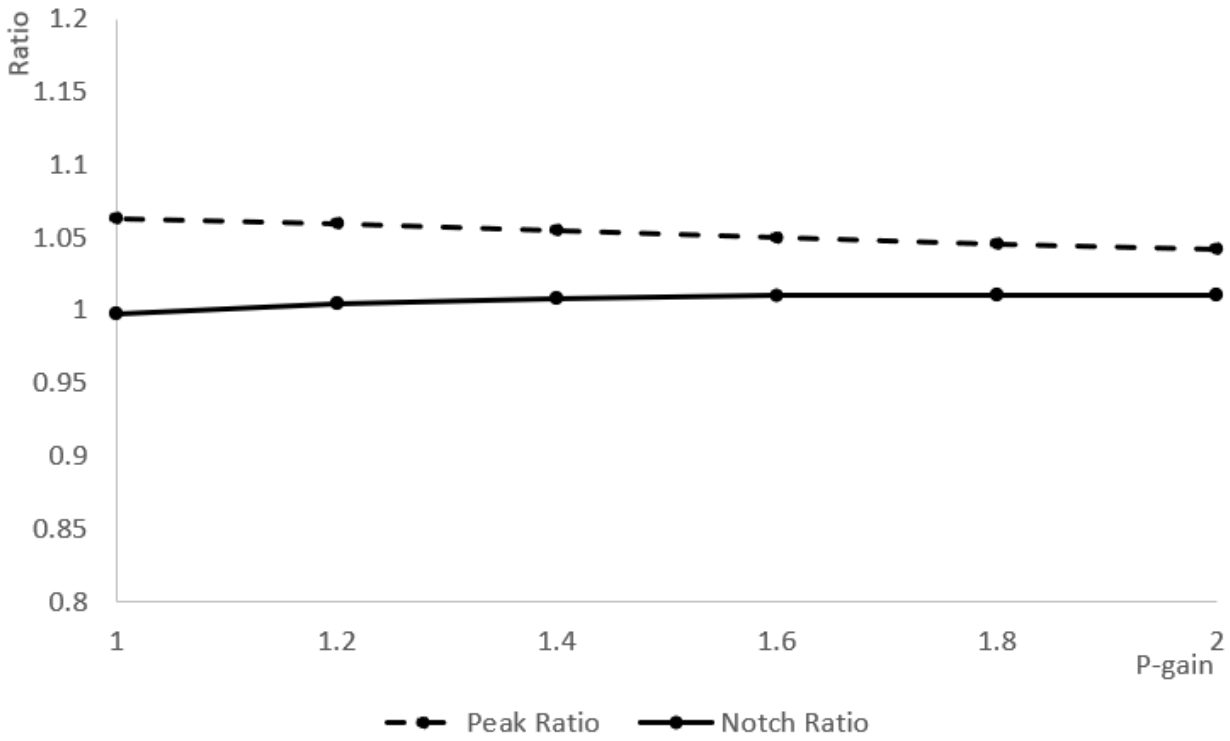

Figure 5.21 Effects of changing Proportional gain on peak and notch value for NBUT's model loaded with 1 Hz SDOF structure

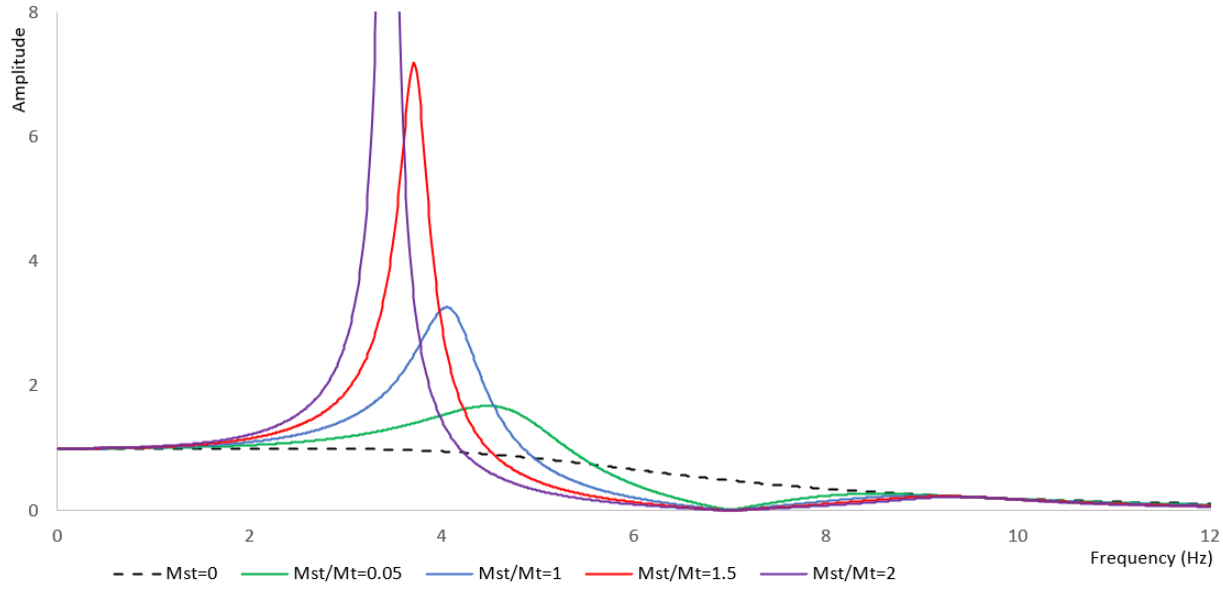

Figure 5.22 Effects of changing structural mass for NBUT's model loaded with 7 Hz SDOF structure

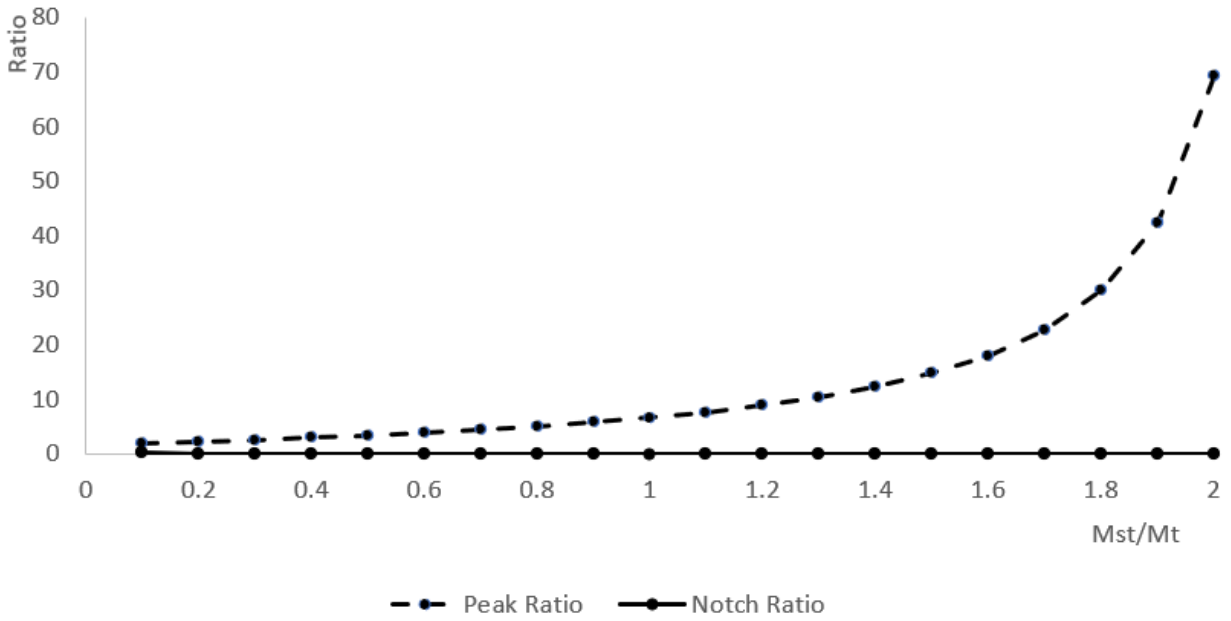

Figure 5.23 Effects of changing structural mass on peak and notch value for NBUT's model loaded with 7 Hz SDOF structure

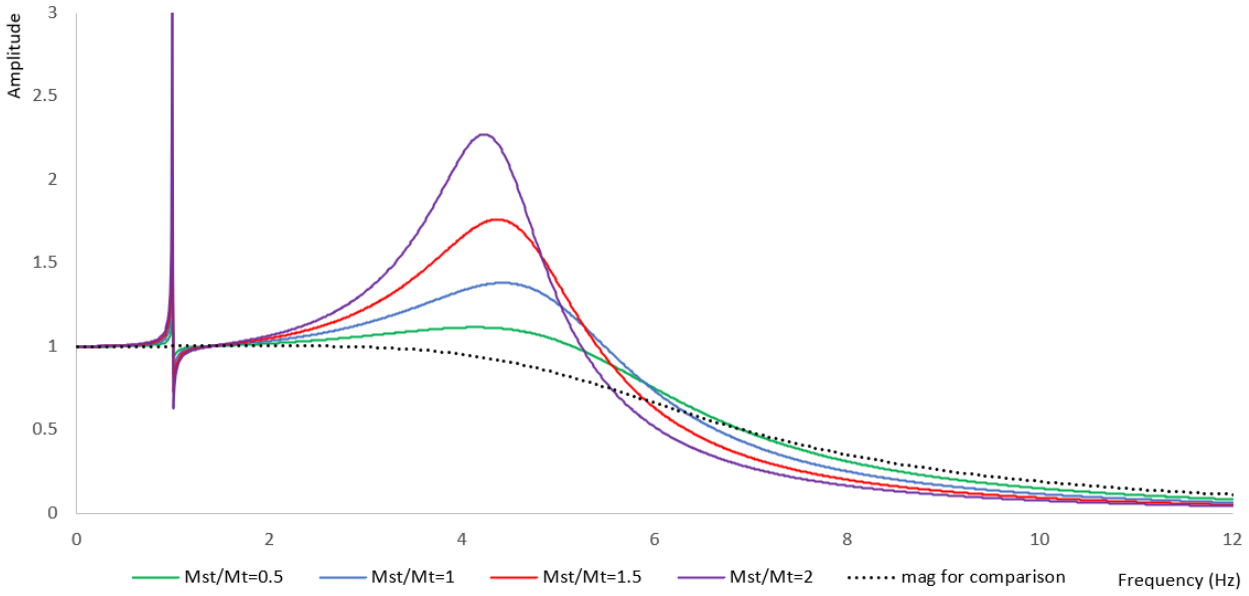

Figure 5.24 Effects of changing structural mass for NBUT's model loaded with 1 Hz SDOF structure

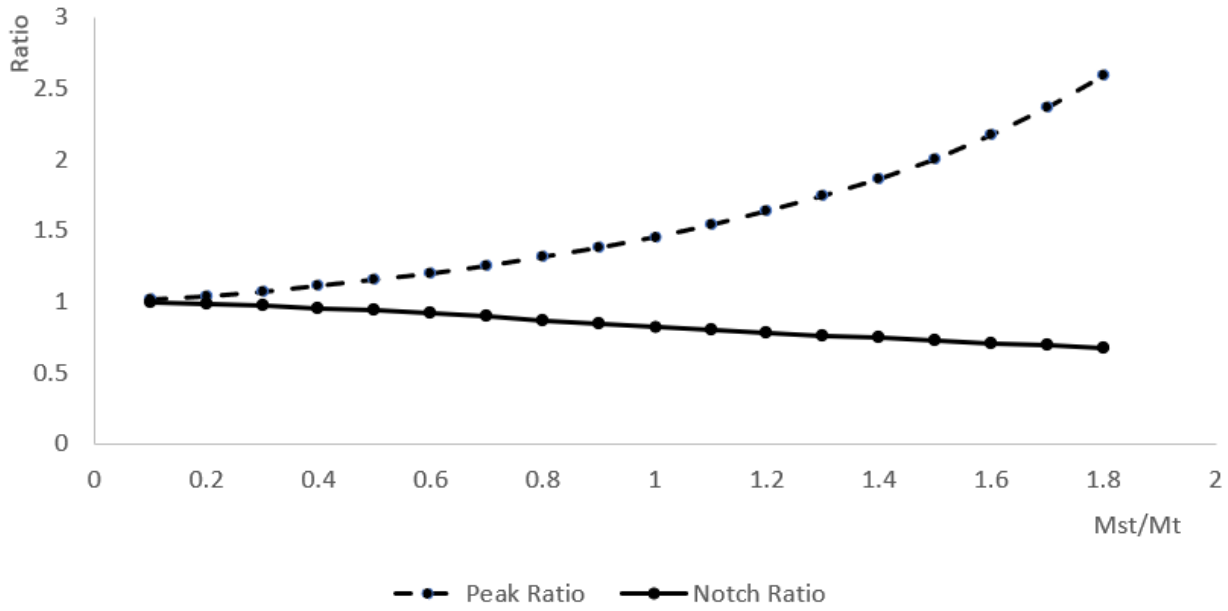

Figure 5.25 Effects of changing structural mass on peak and notch value for NBUT's model loaded with 1 Hz SDOF structure

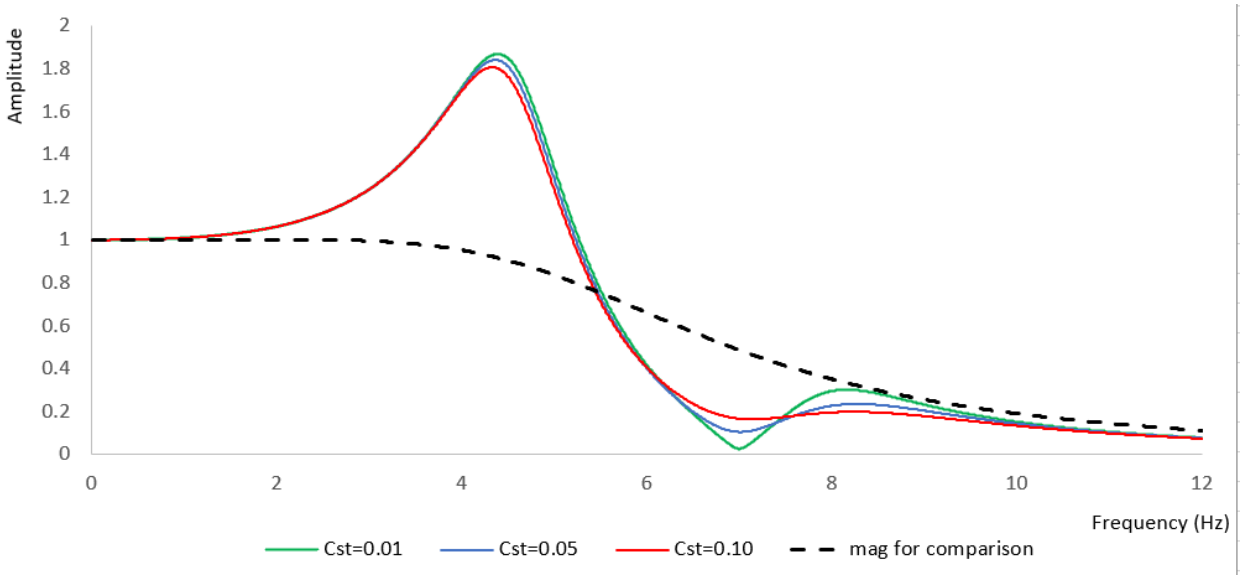

Figure 5.26 Effects of changing structural damping for NBUT's model loaded with 7 Hz SDOF structure

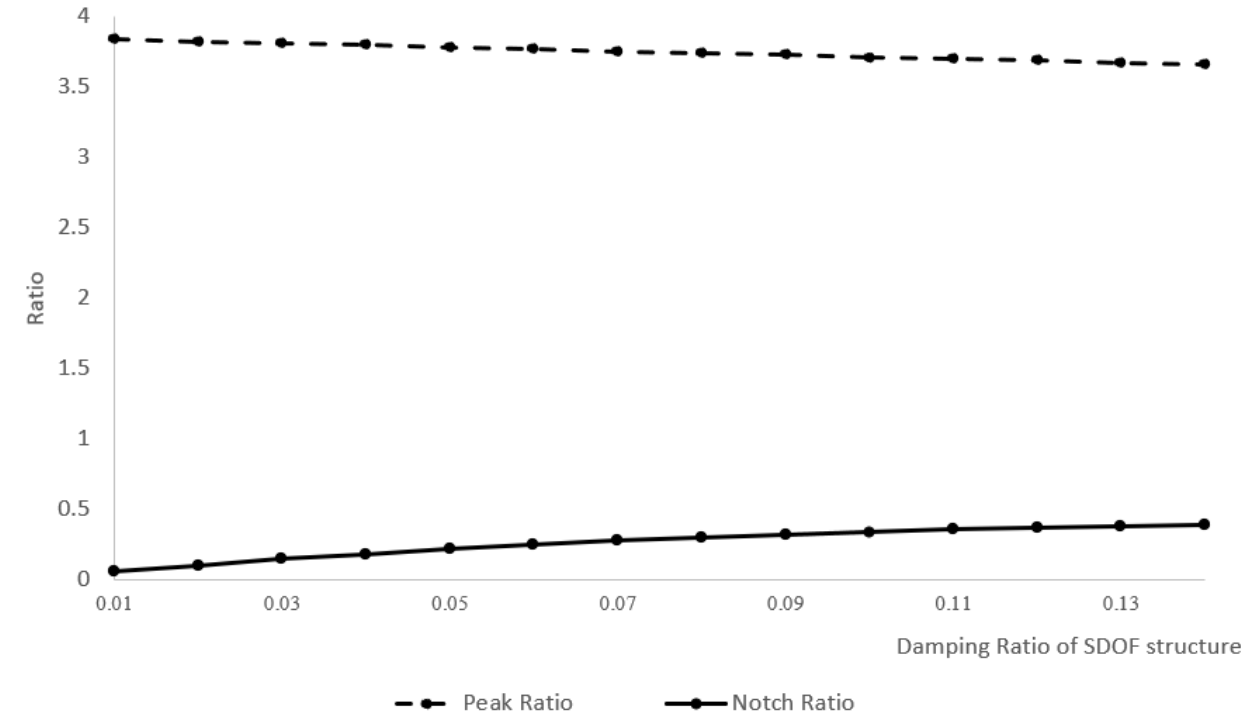

Figure 5.27 Effects of changing structural damping on peak and notch value for NBUT's model loaded with 7 Hz SDOF structure

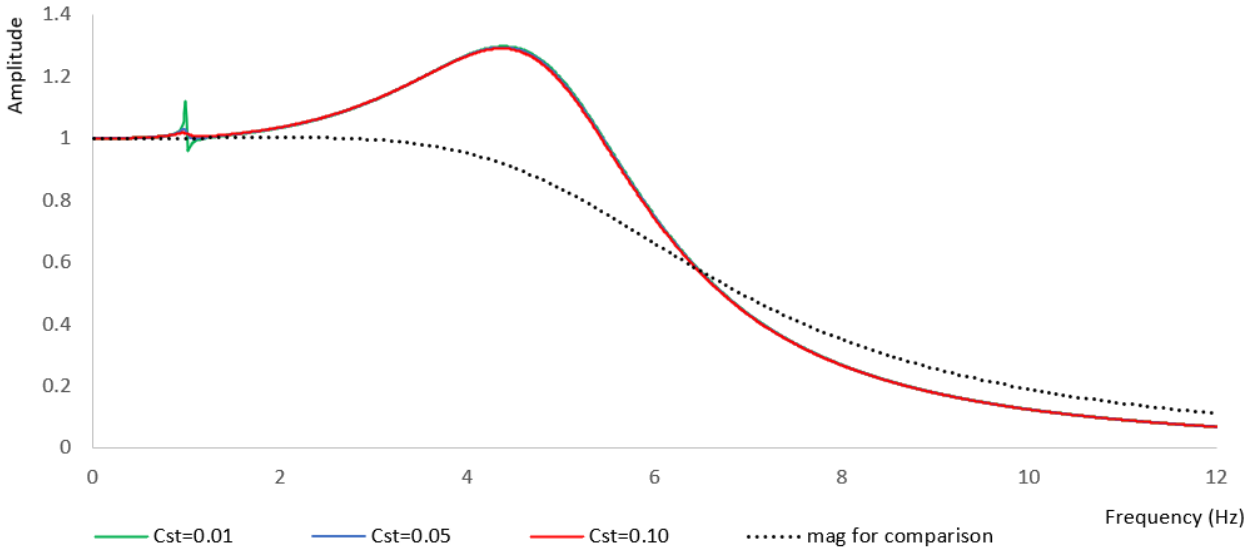

Figure 5.28 Effects of changing structural damping for NBUT's model loaded with 1 Hz SDOF structure

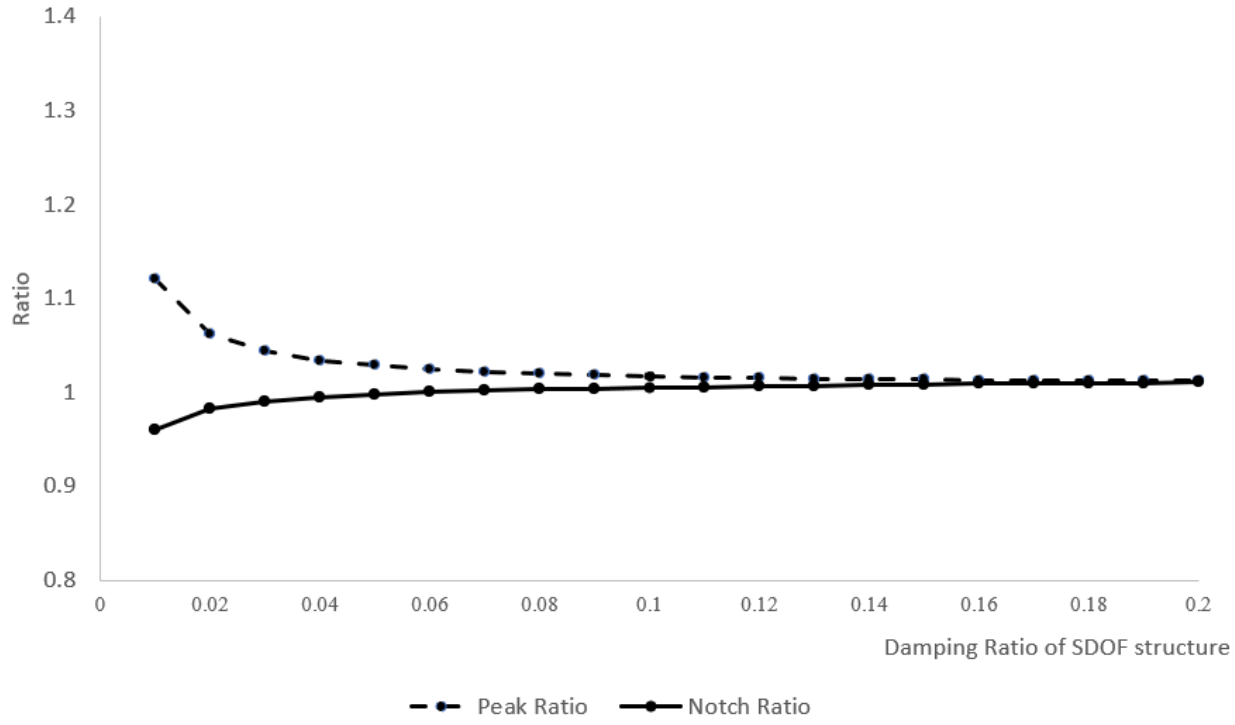

Figure 5.29 Effects of changing structural damping on peak and notch value for NBUT's model loaded with 7 Hz SDOF structure

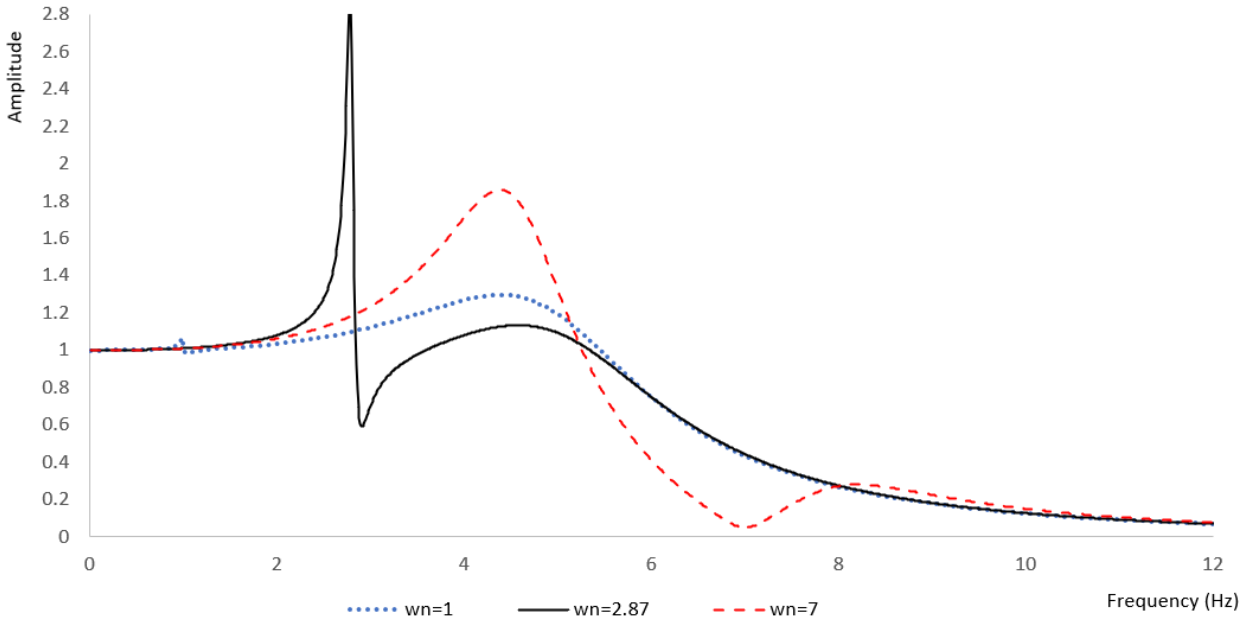

Figure 5.30 Different natural frequency of structures in NBUT's shake table system

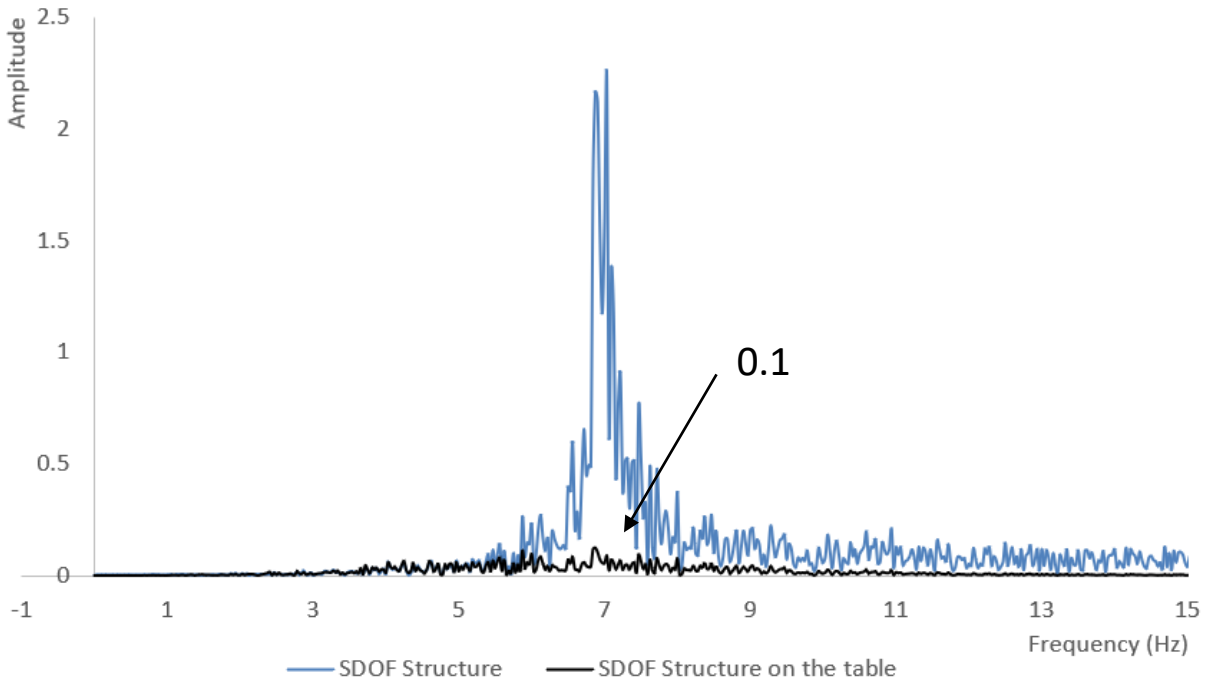

Figure 5.31 FFT response of SDOF structural displacement on the ground and SDOF structural relative displacement mounted on the table for NBUT's table in nonlinear system

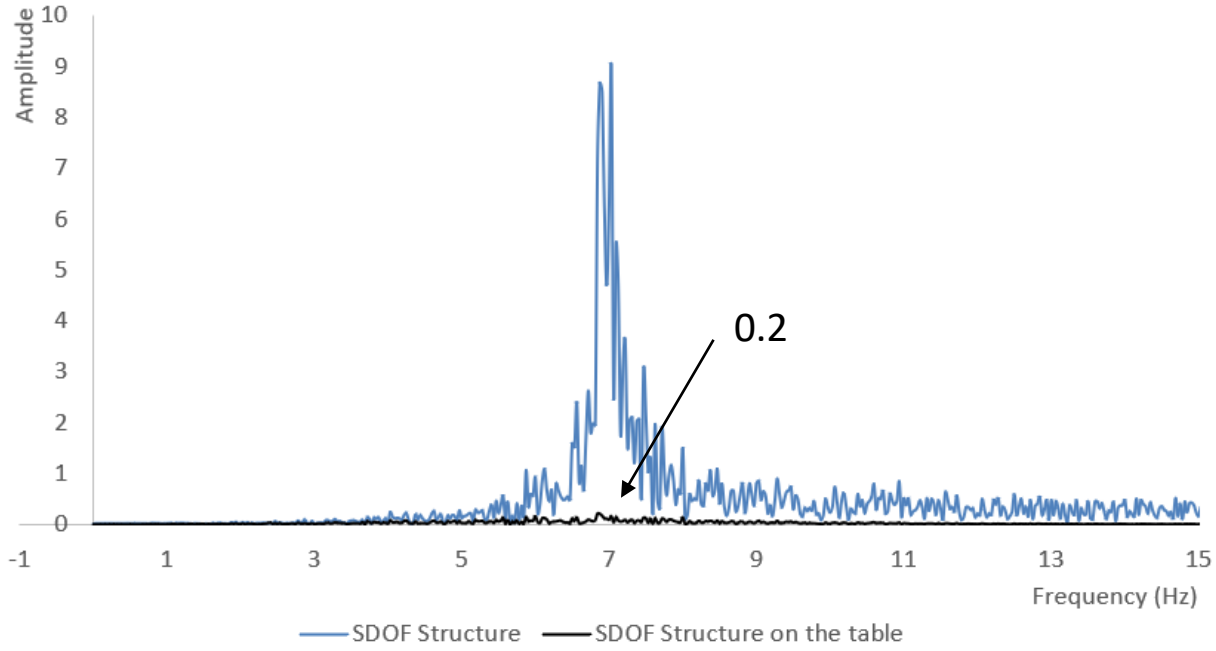

Figure 5.32 FFT response of SDOF structural displacement on the ground and SDOF structural relative displacement mounted on the table for NBUT's table in nonlinear system (4 times input)